International Journal of Advanced Engineering and Technology Research
ISSN: 3106-8677 (Print), ISSN: 3106-8685 (Online) | Vol. 2, No. 1, 2026

An Efficient Legendre Polynomial Series Approach for Thermoelastic Waves in Functionally Graded Piezoelectric Nano Hollow Cylinder

Xian Luo

School of Mechanical and Power Engineering, Henan Polytechnic University, Jiaozuo 454003, China
18000740185@163.com

Abstract: The Legendre polynomial series approach (LPSA) has the advantages of simple derivation process, high solving efficiency, and small computational scale, making it an efficient method for solving wave mechanics. However, when solving the nonlocal nano hollow cylindrical structure, the nonlocal integral elastic relationship makes it consume extremely much CPU time for integrals containing the reciprocal of radius, Legendre polynomials, absolute values, and exponential function. To overcome this drawback, an efficiently iterative solution method by using the exponential integral function are proposed to solve these difficult to calculate analytically and time-consuming integrals. Then, a mathematical model is established for axial thermoelastic wave propagation and attenuation in functionally graded piezoelectric nano hollow cylinders based on the presented LPSA and modified nonlocal integral elasticity. The coupling effects of nonlocal parameter, circumferential order, piezoelectric effect, and gradient index on wave characteristics are studied. Numerical results show that both the thermal wave and elastic wave are size-dependent. The nonlocal effect decreases the phase velocity of thermal waves and elastic waves. Meanwhile, it increases the attenuation of thermal waves, but decreases the attenuation of elastic waves. For the phase velocity, the nonlocal effect and circumferential order are mutually reinforcing, although the nonlocal effect and piezoelectric effect are mutually inhibiting.

Keywords: Thermoelastic waves, modified nonlocal integral elasticity, Legendre polynomials, functionally graded piezoelectric material, attenuation.

1. Introduction

Piezoelectric nano hollow cylindrical structures have broad application prospects in MEMS such as acoustic devices [1]. And the elastic wave characteristics are the theoretical basis for the design and optimization of MEMS. However, the scale effect [2] in nanostructures poses significant difficulties in solving the wave propagation in piezoelectric hollow cylindrical structures.

As an important theory for studying the scale effect, nonlocal integral elasticity (NIE) [3] introduces an integral function that includes reciprocal of radius, exponential term, and absolute value. This integral function effectively expresses the nonlocal assumption that the stress is not only related to the strain at that point, but also to the strain at other points in the structure. Unfortunately, it also leads to the inability to analytically calculate the integration in existing wave dynamics methods, resulting in excessively long numerical integration time and serious computational efficiency problems [4]. In order to reduce the difficulty of solving nanostructures, the nonlocal differential elasticity, which is an approximation of the original nonlocal integral one, is used in many papers [5-8]. However, there is a remarkable difference between the results from nonlocal integral and differential elasticity [9-11]. This leads to unreliable results from nonlocal differential elasticity in acoustic device design. Therefore, developing an efficient solution method to study the wave propagation in nonlocal integral elastic piezoelectric hollow cylindrical structures is of great significance for wave performance regulation in acoustic devices.

In the piezoelectric nanostructures, elastic waves are endowed with some new characteristics by the scale effect, such as modal compression [12], existence of escape frequency [13], increased dissipation of plane waves [9], et al. Such phenomena can be used to develop various wave devices. For instance, the clamping loss caused by elastic waves under the scale effect can be considered in designing the microresonators [14]. For the demand of nanoacoustic device design, Yan et al. [15] considered the transverse elastic wave in periodic piezoelectric nonlocal nano laminates with defects. Li et al. [16] analyzed wave behaviors in porous FGPM nonlocal strain gradient nanoplates deposited in a viscoelastic foundation with thermoelectric loads. Li et al. [17] investigated the SH waves in piezoelectric semiconductor nanoplates with surface effect. Singh et al. [18] studied the plane wave propagation in an interface between two different micropolar piezoelectric half-spaces. All above papers considered piezoelectric plate structures. For the nano hollow cylinder, Ghayoumizadeh et al. [19] considered the transient dynamic analysis of elastic waves in finite-length functionally graded piezoelectric nanocomposites. Wang et al [20] analyzed the circumferential thermoelastic waves in FGM hollow cylinders. He et al. [21] studied wave propagation in FGM elastic nano cylindrical shells by using a nonlocal elastic first-order shear deformation shell model. Daneshman et al. [22] considered the wave propagation behavior in the elastic nano cylindrical shells by applying the third-order shear deformation shell model. Although many papers have investigated the scale effect, the axial wave propagation in piezoelectric nano hollow cylindrical structures with nonlocal integral elasticity is not considered, especially on its attenuation from thermal effect. It is worth noting that acoustic devices often operate in high-temperature environments, and the wave propagation must consider the thermal effect [23, 24].

To solve the wave propagation in hollow cylindrical structures, many methods are presented, such as the scaled boundary finite element method [25], the normal mode expansion method [26], the generalized differential quadrature and Newmark approach [27], the meshless method [19, 28], the boundary element method [29], the global matrix method [30], and the Legendre polynomial series approach (LPSA) [31, 32], etc. Among them, the LPSA has the advantages of simple derivation process, high solving efficiency, and small computational scale, and has been updated several times to solve different wave problems. Lefebvre et al. [33] first used the LPSA to study the wave characteristics in multilayered and FGM plate structures. Elmaimouni et al. [34] studied wave propagation in FGM hollow cylinders by using the LPSA. Yu et al. [35] improved the LPSA to over the physical field discontinuity problem by using the classical LPSA. Zheng et al. [36] coupled state vector and LPSA to solve the wave propagation. Wang et al. [6] developed the LPSA with a bidirectional iterative integration technique for the nonlocal integral nano plate structures. However, when solving wave propagation in nano hollow cylindrical structures, the LPSA contains integrals with the reciprocal of radius, Legendre polynomials, absolute values, and exponential functions. These new integral forms make numerical solutions more difficult and seriously affect the computational ability.

In this paper, the MNIE-LPSA is developed to investigate the thermoelastic guided wave propagation in functionally graded piezoelectric material (FGPM) nano hollow cylinders by using the modified nonlocal integral elasticity (MNIE) [37]. The MNIE improves the inappropriateness of the stress assumption in classical nonlocal integral elasticity for FGM nanostructures. To overcome the numerical integration difficulty in solving nonlocal integral elasticity, the iterative integral solving technique is proposed by using the exponential integral functions and Legendre series expansion. The computational efficiency is greatly improved. The phase velocity and attenuation of thermoelastic waves in FGPM nano hollow cylinders are investigated by considering the coupling effects of nonlocal elasticity and other important parameters.

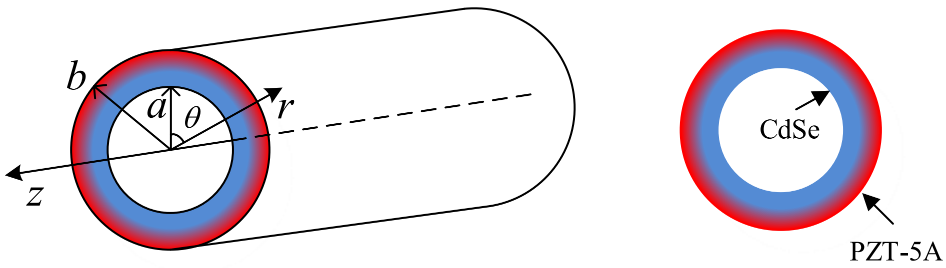

(a) The model of nano hollow cylinder; (b) Material components

Figure 1. Functionally graded nonlocal nano hollow cylinder

2. Mathematical Model and Solving Process

Fig.1(a) shows a FGPM nano cylindrical shell in Cylinder Coordinate system (r, θ, z). Its inner and outer radius are a and b (b>a>0), respectively. The thickness is h=b-a. And its graded distribution is in the r-direction. The wave propagates at the z-direction. The FGM is composed of CdSe inside and PZT-5A outside, as shown in Fig. 1(b).

According to the MNIE [37] and the LS theory [38], the governing equations are:

$$\frac{\partial \sigma_{rr}}{\partial r}+\frac{1}{r}\frac{\partial \sigma_{r\theta}}{\partial \theta}+\frac{\partial \sigma_{rz}}{\partial z}+\frac{\sigma_{rr}-\sigma_{\theta\theta}}{r}=\rho\frac{\partial^2 u_r}{\partial t^2}$$

$$\frac{\partial \sigma_{r\theta}}{\partial r}+\frac{1}{r}\frac{\partial \sigma_{\theta\theta}}{\partial \theta}+\frac{\partial \sigma_{\theta z}}{\partial z}+\frac{2\sigma_{r\theta}}{r}=\rho\frac{\partial^2 u_\theta}{\partial t^2}$$

$$\frac{\partial \sigma_{rz}}{\partial r}+\frac{1}{r}\frac{\partial \sigma_{\theta z}}{\partial \theta}+\frac{\partial \sigma_{zz}}{\partial z}+\frac{\sigma_{rz}}{r}=\rho\frac{\partial^2 u_z}{\partial t^2}$$

$$\frac{\partial D_r}{\partial r}+\frac{1}{r}\frac{\partial D_\theta}{\partial \theta}+\frac{\partial D_z}{\partial z}+\frac{D_r}{r}=0$$

$$K_1\frac{\partial^2 T}{\partial r^2}+K_2\left(\frac{1}{r^2}\frac{\partial^2 T}{\partial \theta^2}+\frac{1}{r}\frac{\partial T}{\partial r}\right)+K_3\frac{\partial^2 T}{\partial z^2}=$$
$$\left(1+\frac{\partial}{\partial t}\right)\left(\rho C_e\frac{\partial \chi}{\partial t}+T_0\beta_1\frac{\partial \varepsilon_{rr}}{\partial t}+T_0\beta_2\frac{\partial \varepsilon_{\theta\theta}}{\partial t}+T_0\beta_3\frac{\partial \varepsilon_{zz}}{\partial t}+T_0P_3\frac{\partial E_z}{\partial t}\right) \tag{1a~e}$$

Here D_j is the component electric displacements, respectively. ϕ is the electric potential. T and χ indicate the local and nonlocal temperature variation, respectively; $T=[\chi]_{nl}$. ρ is the material density. t and t0 indicate the time and relaxation time.

The constitutive relations are

$$\begin{cases}\sigma_{ij}=C_{ijkl}\varepsilon_{kl}-e_{jk}E_k-\beta_j T\\ D_j=e_{jkl}\varepsilon_{kl}+\in_{jk}E_k+P_jT\end{cases} \tag{2}$$

Where C_{ijkl}, e_{jk}, β_j and $\in_{jk}$ are the elastic constants, piezoelectric constants and volume expanding coefficients, respectively. E_k denote the electric field intensity.

Referring to the MNIE [37], the geometric relations are

$$\varepsilon_{rr}=\left[\frac{\partial u_r}{\partial r}\right]_{nl},\qquad \varepsilon_{\theta\theta}=\left[\frac{1}{r}\frac{\partial u_\theta}{\partial \theta}+\frac{u_r}{r}\right]_{nl},\qquad \varepsilon_{zz}=\left[\frac{\partial u_z}{\partial z}\right]_{nl},$$
$$\varepsilon_{\theta z}=\frac{1}{2}\left[\frac{\partial u_\theta}{\partial z}+\frac{1}{r}\frac{\partial u_z}{\partial \theta}\right]_{nl}\quad \varepsilon_{r\theta}=\frac{1}{2}\left[\frac{1}{r}\frac{\partial u_r}{\partial \theta}+\frac{\partial u_\theta}{\partial r}-\frac{u_\theta}{r}\right]_{nl}\quad \varepsilon_{rz}=\frac{1}{2}\left[\frac{\partial u_r}{\partial z}+\frac{\partial u_z}{\partial r}\right]_{nl} \tag{3}$$
$$E_r=-\left[\frac{\partial \phi}{\partial r}\right]_{nl},\qquad E_\theta=-\left[\frac{1}{r}\frac{\partial \phi}{\partial \theta}\right]_{nl},\qquad E_z=-\left[\frac{\partial \phi}{\partial z}\right]_{nl}$$

$[\mathrm{g}]_{nl}=\int_a^b \alpha\left(|r-v|,\lambda\right)\bullet dv$, and λ is the nonlocal parameter [4]. The nonlocal factor is

$$\alpha(|r-v|,\lambda)=\frac{1}{2\lambda}\exp\left(-\frac{|r-v|}{\lambda}\right) \tag{4}$$

The electrical boundary conditions are

$$\begin{cases} D_r\big|_{r=a,b}=0, & \text{open-circuit} \\ \phi\big|_{r=a,b}=0, & \text{closed-circuit} \end{cases} \tag{5}$$

The isothermal boundary condition is

$$\left.\frac{\partial T}{\partial r}\right|_{r=a,b}=0 \tag{6}$$

Assuming $v_z=\sqrt{\bar{C}_{11}/\bar{\rho}}$ and $k_z=\bar{K}_1/\bar{\rho}\bar{C}_e$, the dimensionless can be implemented by the following transformation,

$$\hat{C}_{ij}=\frac{C_{ij}}{\bar{C}_{11}},\qquad \hat{\rho}=\frac{\rho}{\bar{\rho}},\qquad \hat{x}_i=\frac{v_z}{k_z}x_i,\quad \hat{u}_i=\frac{v_x^3\bar{\rho}}{k_x\bar{\beta}_1T_0}u_i,\quad \hat{t}_0=\frac{v_z^2}{k_z}t_0,$$
$$\eta=\frac{\left(\bar{\beta}_1\right)^2T_0}{\bar{\rho}^2\bar{C}_e v_z^2},\quad \hat{\Phi}=\frac{v_z\bar{e}_{33}}{k_z\bar{\beta}_1T_0}\Phi,\quad \hat{P}_i=\frac{P_i\bar{C}_{11}}{\bar{\beta}_1\bar{e}_{33}},\quad \hat{\in}_{ij}=\frac{\in_{ij}\bar{C}_{11}}{\left(\bar{e}_{33}\right)^2},\quad \hat{e}_{ij}=\frac{e_{ij}}{\bar{e}_{33}}, \tag{7}$$
$$\hat{T}=\frac{T}{T_0},\qquad \hat{\beta}_i=\frac{\beta_i}{\bar{\beta}_1},\qquad \hat{K}_i=\frac{K_i}{\bar{K}_1},\qquad \hat{C}_e=\frac{C_e}{\bar{C}_e},\qquad \hat{\lambda}=\frac{\lambda}{h}$$

The contracting subscript notations are used (11→1, 22→2, 33→3, 23→4, 13→5, 12→6) to relate to C_{ijkl} to C_{mn}, where i, j, k, l=1, 2, 3; and m, n=1, 2, 3, 4, 5, 6.

2.1. Electrical Open-Circuit Condition

Bringing Eqs. (2)-(7) into the governing equation (1), considering the electrical open-circuit and traction-free boundary conditions, and rewriting $\hat{\bullet}$ to $\bullet$, one has

$$\begin{aligned}
&\frac{\partial}{\partial r}\left(C_{11}\left[\frac{\partial u_r}{\partial r}\right]_{nl}\right)+\frac{\partial}{\partial r}\left(C_{12}\left[\frac{u_r}{r}\right]_{nl}\right)+C_{11}\left[\frac{\partial u_r}{\partial r}\right]_{nl}\frac{\partial H(r)}{\partial r}+C_{12}\left[\frac{u_r}{r}\right]_{nl}\frac{\partial H(r)}{\partial r}-\frac{\partial}{\partial r}\left(\beta_1[\chi]_{nl}\right)\\
&+C_{66}\frac{1}{r}\frac{\partial}{\partial \theta}\left[\frac{1}{r}\frac{\partial u_r}{\partial \theta}\right]_{nl}+C_{55}\frac{\partial}{\partial z}\left[\frac{\partial u_r}{\partial z}\right]_{nl}+\frac{1}{r}\left\{\left(C_{11}-C_{12}\right)\left[\frac{\partial u_r}{\partial r}\right]_{nl}+\left(C_{12}-C_{22}\right)\left[\frac{u_r}{r}\right]_{nl}\right\}-\rho\frac{\partial^2 u_r}{\partial t^2}\\
&+\frac{\partial}{\partial r}\left(C_{12}\left[\frac{1}{r}\frac{\partial u_\theta}{\partial \theta}\right]_{nl}\right)+C_{12}\left[\frac{1}{r}\frac{\partial u_\theta}{\partial \theta}\right]_{nl}\frac{\partial H(r)}{\partial r}+C_{66}\frac{1}{r}\frac{\partial}{\partial \theta}\left[\frac{\partial u_\theta}{\partial r}-\frac{u_\theta}{r}\right]_{nl}+\frac{C_{12}-C_{22}}{r}\left[\frac{1}{r}\frac{\partial u_\theta}{\partial \theta}\right]_{nl}\\
&+\frac{\partial}{\partial r}\left(C_{13}\left[\frac{\partial u_z}{\partial z}\right]_{nl}\right)+C_{13}\left[\frac{\partial u_z}{\partial z}\right]_{nl}\frac{\partial H(r)}{\partial r}+C_{55}\frac{\partial}{\partial z}\left[\frac{\partial u_z}{\partial r}\right]_{nl}+\frac{C_{13}-C_{23}}{r}\left[\frac{\partial u_z}{\partial z}\right]_{nl}-\beta_1[\chi]_{nl}\frac{\partial H(r)}{\partial r}\\
&+\frac{\partial}{\partial r}\left(e_{31}\left[\frac{\partial \Phi}{\partial z}\right]_{nl}\right)+e_{31}\left[\frac{\partial \Phi}{\partial z}\right]_{nl}\frac{\partial H(r)}{\partial r}+e_{15}\frac{\partial}{\partial z}\left[\frac{\partial \Phi}{\partial r}\right]_{nl}+\frac{e_{31}-e_{32}}{r}\left[\frac{\partial \Phi}{\partial z}\right]_{nl}+\frac{\beta_2-\beta_1}{r}[\chi]_{nl}=0
\end{aligned}$$

$$
\begin{aligned}
&\frac{\partial}{\partial r}\left(C_{66}\left[\frac{1}{r}\frac{\partial u_r}{\partial \theta}\right]_{nl}\right)+C_{66}\left[\frac{1}{r}\frac{\partial u_r}{\partial \theta}\right]_{nl}\frac{\partial H(z)}{\partial r}+C_{12}\frac{1}{r}\frac{\partial}{\partial \theta}\left[\frac{\partial u_r}{\partial r}\right]_{nl}+C_{22}\frac{1}{r}\frac{\partial}{\partial \theta}\left[\frac{u_r}{r}\right]_{nl}+C_{22}\frac{2}{r}\left[\frac{1}{r}\frac{\partial u_r}{\partial \theta}\right]_{nl}\\
&+C_{66}\frac{\partial}{\partial r}\left[\frac{\partial u_\theta}{\partial r}-\frac{u_\theta}{r}\right]_{nl}+C_{66}\left[\frac{\partial u_\theta}{\partial r}-\frac{u_\theta}{r}\right]_{nl}\frac{\partial H(z)}{\partial r}+C_{22}\frac{1}{r}\frac{\partial}{\partial \theta}\left[\frac{1}{r}\frac{\partial u_\theta}{\partial \theta}\right]_{nl}\\
&+C_{44}\frac{\partial}{\partial z}\left[\frac{\partial u_\theta}{\partial z}\right]_{nl}+\frac{2}{r}C_{66}\left[\frac{\partial u_\theta}{\partial r}-\frac{u_\theta}{r}\right]_{nl}-\rho\frac{\partial^2 u_\theta}{\partial t^2}\\
&-\rho\frac{\partial^2 u_\theta}{\partial t^2}+C_{23}\frac{1}{r}\frac{\partial}{\partial \theta}\left[\frac{\partial u_z}{\partial z}\right]_{nl}+C_{44}\frac{\partial}{\partial z}\left[\frac{1}{r}\frac{\partial u_z}{\partial \theta}\right]_{nl}+e_{32}\frac{1}{r}\frac{\partial}{\partial \theta}\left[\frac{\partial \phi}{\partial z}\right]_{nl}+e_{24}\frac{\partial}{\partial z}\left[\frac{1}{r}\frac{\partial \phi}{\partial \theta}\right]_{nl}-\beta_2\frac{1}{r}\frac{\partial[\chi]_{nl}}{\partial \theta}=0
\end{aligned}
$$

$$
\begin{aligned}
&\frac{\partial}{\partial r}\left(C_{55}\left[\frac{\partial u_r}{\partial z}\right]_{nl}\right)+C_{55}\left[\frac{\partial u_r}{\partial z}\right]_{nl}\frac{\partial H(z)}{\partial r}+C_{55}\frac{1}{r}\left[\frac{\partial u_r}{\partial z}\right]_{nl}+C_{13}\frac{\partial}{\partial z}\left[\frac{\partial u_r}{\partial r}\right]_{nl}+C_{23}\frac{\partial}{\partial z}\left[\frac{u_r}{r}\right]_{nl}\\
&+C_{44}\frac{1}{r}\frac{\partial}{\partial \theta}\left[\frac{\partial u_\theta}{\partial z}\right]_{nl}+C_{23}\frac{1}{r}\frac{\partial}{\partial z}\left[\frac{\partial u_\theta}{\partial \theta}\right]_{nl}-\beta_3\frac{\partial[\chi]_{nl}}{\partial z}-\rho\frac{\partial^2 u_z}{\partial t^2}\\
&+\frac{\partial}{\partial r}\left(C_{55}\left[\frac{\partial u_z}{\partial r}\right]_{nl}\right)+C_{55}\left[\frac{\partial u_z}{\partial r}\right]_{nl}\frac{\partial H(z)}{\partial r}+C_{44}\frac{1}{r}\frac{\partial}{\partial \theta}\left[\frac{1}{r}\frac{\partial u_z}{\partial \theta}\right]_{nl}+C_{55}\frac{1}{r}\left[\frac{\partial u_z}{\partial r}\right]_{nl}+C_{33}\frac{\partial}{\partial z}\left[\frac{\partial u_z}{\partial z}\right]_{nl}\\
&+\frac{\partial}{\partial r}\left(e_{15}\left[\frac{\partial \Phi}{\partial r}\right]_{nl}\right)+e_{15}\left[\frac{\partial \Phi}{\partial r}\right]_{nl}\frac{\partial H(z)}{\partial r}+e_{24}\frac{1}{r}\frac{\partial}{\partial \theta}\left[\frac{1}{r}\frac{\partial \Phi}{\partial \theta}\right]_{nl}+e_{15}\frac{1}{r}\left[\frac{\partial \Phi}{\partial r}\right]_{nl}+e_{33}\frac{\partial}{\partial z}\left[\frac{\partial \Phi}{\partial z}\right]_{nl}=0
\end{aligned}
$$

$$
\begin{aligned}
&\frac{\partial}{\partial r}\left(e_{15}\left[\frac{\partial u_r}{\partial z}\right]_{nl}\right)+e_{15}\left[\frac{\partial u_r}{\partial z}\right]_{nl}\frac{\partial H(z)}{\partial r}+e_{31}\frac{\partial}{\partial z}\left[\frac{\partial u_r}{\partial r}\right]_{nl}+e_{32}\frac{\partial}{\partial z}\left[\frac{u_r}{r}\right]_{nl}+e_{15}\frac{1}{r}\left[\frac{\partial u_r}{\partial z}\right]_{nl}\\
&+e_{32}\frac{\partial}{\partial z}\left[\frac{1}{r}\frac{\partial u_\theta}{\partial \theta}\right]_{nl}+e_{24}\frac{1}{r}\frac{\partial}{\partial \theta}\left[\frac{\partial u_\theta}{\partial z}\right]_{nl}+\frac{\partial P_3}{\partial r}[\chi]_{nl}+P_3\frac{\partial}{\partial r}[\chi]_{nl}+P_3[\chi]_{nl}\frac{\partial H(z)}{\partial r}+P_3\frac{1}{r}[\chi]_{nl}\\
&+\frac{\partial}{\partial r}\left(e_{15}\left[\frac{\partial u_z}{\partial r}\right]_{nl}\right)+e_{15}\left[\frac{\partial u_z}{\partial r}\right]_{nl}\frac{\partial H(z)}{\partial r}+e_{33}\frac{\partial}{\partial z}\left[\frac{\partial u_z}{\partial z}\right]_{nl}+e_{15}\frac{1}{r}\left[\frac{\partial u_z}{\partial r}\right]_{nl}+e_{24}\frac{1}{r}\frac{\partial}{\partial \theta}\left[\frac{1}{r}\frac{\partial u_z}{\partial \theta}\right]_{nl}\\
&-\frac{\partial}{\partial r}\left(\in_{11}\left[\frac{\partial \Phi}{\partial r}\right]_{nl}\right)-\in_{11}\left[\frac{\partial \Phi}{\partial r}\right]_{nl}\frac{\partial H(z)}{\partial r}-\in_{33}\frac{\partial}{\partial z}\left[\frac{\partial \Phi}{\partial z}\right]_{nl}-\in_{11}\frac{1}{r}\left[\frac{\partial \Phi}{\partial r}\right]_{nl}-\in_{22}\frac{1}{r}\frac{\partial}{\partial \theta}\left[\frac{1}{r}\frac{\partial \Phi}{\partial \theta}\right]_{nl}=0
\end{aligned}
$$

$$
\begin{aligned}
&K_1\frac{\partial^2[\chi]_{nl}}{\partial r^2}+K_2\left(\frac{1}{r^2}\frac{\partial^2[\chi]_{nl}}{\partial \theta^2}+\frac{1}{r}\frac{\partial[\chi]_{nl}}{\partial r}\right)+K_3\frac{\partial^2[\chi]_{nl}}{\partial z^2}-\rho C_e\frac{\partial}{\partial t}\left(1+\frac{\partial}{\partial t}\right)\chi+T_0P_3\frac{\partial}{\partial t}\left(1+\frac{\partial}{\partial t}\right)\frac{\partial}{\partial z\partial t}[\phi]_{nl}=\\
&+T_0\beta_1\frac{\partial}{\partial t}\left(1+\frac{\partial}{\partial t}\right)\frac{\partial}{\partial t}\left[\frac{\partial u_r}{\partial r}\right]_{nl}+T_0\beta_2\frac{\partial}{\partial t}\left(1+\frac{\partial}{\partial t}\right)\frac{\partial}{\partial t}\left[\frac{1}{r}\frac{\partial u_\theta}{\partial \theta}+\frac{u_r}{r}\right]_{nl}+T_0\beta_3\frac{\partial}{\partial t}\left(1+\frac{\partial}{\partial t}\right)\frac{\partial}{\partial t}\left[\frac{\partial u_z}{\partial z}\right]_{nl}
\end{aligned}
\tag{8a~e}
$$

The electrical open-circuit and traction-free boundary conditions are shown as

$$
\begin{cases}\sigma_{rj}=\sigma_{rj}H(r)\\ D_r=D_rH(r)\end{cases}\tag{9}
$$

and

$$
H(r)=\begin{cases}1, & a\le r\le b\\ 0, & else\end{cases}\tag{10}
$$

For the harmonic wave propagation in the z-direction, one has

$$
\{u_r,\,u_\theta,\,u_z,\,\varPhi,\,\chi,\,T\}=\{U(r),\,V(r),\,W(r),\,X(r),\,Y(r),\,Z(r)\}\exp(ikz+iN\theta-i\omega t)\tag{11}
$$

Additionally, the material parameters can be expanded as the following L-order polynomial series,

$$C_{ij}(r)=C_{ij}^{(l)}\left(\frac{2r-(b+a)}{b-a}\right)^l,\rho_i(r)=\rho_i^{(l)}\left(\frac{2r-(b+a)}{b-a}\right)^l,e_{ij}(r)=e_{ij}^{(m)}\left(\frac{2r-(b+a)}{b-a}\right)^l,$$

$$\in_{ij}(r)=\in_{ij}^{(l)}\left(\frac{2r-(b+a)}{b-a}\right)^l,K_i(r)=K_i^{(l)}\left(\frac{2r-(b+a)}{b-a}\right)^l,\beta_i(r)=\beta_i^{(m)}\left(\frac{2r-(b+a)}{b-a}\right)^l,\ \text{l=0, 1, 2, ..., L.}\quad(12)$$

$$C_e(r)=C_e^{(l)}\left(\frac{2r-(b+a)}{b-a}\right)^l,\quad P_i(r)=P_i^{(l)}\left(\frac{2r-(b+a)}{b-a}\right)^l,$$

Introducing Eqs. (1) and (12) into Eq. (8), it yields

$$\begin{aligned}
&-k^2C_{55}[U]_{nl}+\frac{\partial}{\partial r}\left(C_{11}\left[\frac{\partial U}{\partial r}\right]_{nl}\right)+\frac{\partial}{\partial r}\left(C_{12}\left[\frac{U}{r}\right]_{nl}\right)+C_{11}\left[\frac{\partial U}{\partial r}\right]_{nl}\frac{\partial H(r)}{\partial r}+C_{12}\left[\frac{U}{r}\right]_{nl}\frac{\partial H(r)}{\partial r}\\
&+\frac{C_{11}-C_{12}}{r}\left[\frac{\partial U}{\partial r}\right]_{nl}+\frac{C_{12}-C_{22}}{r}\left[\frac{U}{r}\right]_{nl}-N^2C_{66}\frac{1}{r}\left[\frac{U}{r}\right]_{nl}+\omega^2\rho U-\frac{\partial}{\partial r}(\beta_1 Z)-\beta_1 Z\frac{\partial H(r)}{\partial r}\\
&+iN\frac{\partial}{\partial r}\left(C_{12}\left[\frac{V}{r}\right]_{nl}\right)+C_{12}\left[\frac{V}{r}\right]_{nl}\frac{\partial H(r)}{\partial r}+iNC_{66}\frac{1}{r}\left[\frac{\partial V}{\partial r}-\frac{V}{r}\right]_{nl}+iN\frac{C_{12}-C_{22}}{r}\left[\frac{V}{r}\right]_{nl}\\
&+ik\frac{\partial}{\partial r}\left(C_{13}[W]_{nl}\right)+ikC_{13}[W]_{nl}\frac{\partial H(r)}{\partial r}+ikC_{55}\left[\frac{\partial W}{\partial r}\right]_{nl}+ik\frac{C_{13}-C_{23}}{r}[W]_{nl}\\
&+ik\frac{\partial}{\partial r}\left(e_{31}[X]_{nl}\right)+ike_{31}[X]_{nl}\frac{\partial H(r)}{\partial r}+ike_{15}\left[\frac{\partial X}{\partial r}\right]_{nl}+ik\frac{e_{31}-e_{32}}{r}[X]_{nl}+\frac{\beta_2-\beta_1}{r}Z=0
\end{aligned}$$

$$\begin{aligned}
&iN\frac{\partial C_{66}}{\partial r}\left[\frac{U}{r}\right]_{nl}+iNC_{66}\frac{\partial}{\partial r}\left[\frac{U}{r}\right]_{nl}+iNC_{66}\left[\frac{U}{r}\right]_{nl}\frac{\partial H(z)}{\partial r}+iN\frac{1}{r}C_{12}\left[\frac{\partial U}{\partial r}\right]_{nl}+iN\frac{1}{r}C_{22}\left[\frac{U}{r}\right]_{nl}\\
&+iN\frac{2}{r}C_{66}\left[\frac{U}{r}\right]_{nl}-k^2C_{44}[V]_{nl}+\frac{\partial C_{66}}{\partial r}\left[\frac{\partial V}{\partial r}-\frac{V}{r}\right]_{nl}+C_{66}\frac{\partial}{\partial r}\left[\frac{\partial V}{\partial r}-\frac{V}{r}\right]_{nl}+C_{66}\left[\frac{\partial V}{\partial r}-\frac{V}{r}\right]_{nl}\frac{\partial H(z)}{\partial r}\\
&+\frac{2}{r}C_{66}\left[\frac{\partial V}{\partial r}-\frac{V}{r}\right]_{nl}-N^2\frac{1}{r}C_{22}\left[\frac{V}{r}\right]_{nl}+\omega^2\rho V\\
&-kN\frac{1}{r}C_{23}[W]_{nl}-kNC_{44}\left[\frac{W}{r}\right]_{nl}-kN\frac{1}{r}e_{32}[X]_{nl}-kNe_{24}\left[\frac{X}{r}\right]_{nl}-iN\beta_2\frac{Z}{r}=0
\end{aligned}$$

$$\begin{aligned}
&ik\frac{\partial}{\partial r}\left(C_{55}[U]_{nl}\right)+ikC_{55}[U]_{nl}\frac{\partial H(z)}{\partial r}+ikC_{55}\frac{1}{r}[U]_{nl}+ikC_{13}\left[\frac{\partial U}{\partial r}\right]_{nl}+ikC_{23}\left[\frac{U}{r}\right]_{nl}\\
&-kNC_{44}\frac{1}{r}[V]_{nl}-kNC_{23}\left[\frac{V}{r}\right]_{nl}\\
&-k^2C_{33}[W]_{nl}+\frac{\partial}{\partial r}\left(C_{55}\left[\frac{\partial W}{\partial r}\right]_{nl}\right)+C_{55}\left[\frac{\partial W}{\partial r}\right]_{nl}\frac{\partial H(z)}{\partial r}-N^2C_{44}\frac{1}{r}\left[\frac{W}{r}\right]_{nl}+C_{55}\frac{1}{r}\left[\frac{\partial u_z}{\partial r}\right]_{nl}+\rho\omega^2W\\
&-k^2e_{33}[X]_{nl}+\frac{\partial}{\partial r}\left(e_{15}\left[\frac{\partial X}{\partial r}\right]_{nl}\right)+e_{15}\left[\frac{\partial X}{\partial r}\right]_{nl}\frac{\partial H(z)}{\partial r}-N^2e_{24}\frac{1}{r}\left[\frac{X}{r}\right]_{nl}+e_{15}\frac{1}{r}\left[\frac{\partial\Phi}{\partial r}\right]_{nl}-ik\beta_3Z=0
\end{aligned}$$

$$ik\frac{\partial}{\partial r}\left(e_{15}[U]_{nl}\right)+ike_{15}[U]_{nl}\frac{\partial H(z)}{\partial r}+ike_{31}\left[\frac{\partial U}{\partial r}\right]_{nl}+ike_{32}\left[\frac{U}{r}\right]_{nl}+ike_{15}\frac{1}{r}[U]_{nl}$$
$$-kNe_{32}\left[\frac{V}{r}\right]_{nl}-kNe_{24}\frac{1}{r}[V]_{nl}+\frac{\partial P_3}{\partial r}Z+P_3\frac{\partial Z}{\partial r}+P_3Z\frac{\partial H(z)}{\partial r}+P_3\frac{Z}{r}$$
$$-k^2e_{33}[W]_{nl}+\frac{\partial}{\partial r}\left(e_{15}\left[\frac{\partial W}{\partial r}\right]_{nl}\right)+e_{15}\left[\frac{\partial W}{\partial r}\right]_{nl}\frac{\partial H(z)}{\partial r}+e_{15}\frac{1}{r}\left[\frac{\partial W}{\partial r}\right]_{nl}-N^2e_{24}\frac{1}{r}\left[\frac{W}{r}\right]_{nl}$$
$$+k^2\in_{33}[X]_{nl}-\frac{\partial}{\partial r}\left(\in_{11}\left[\frac{\partial X}{\partial r}\right]_{nl}\right)-\in_{11}\left[\frac{\partial X}{\partial r}\right]_{nl}\frac{\partial H(z)}{\partial r}-\in_{11}\frac{1}{r}\left[\frac{\partial X}{\partial r}\right]_{nl}+N^2\in_{22}\frac{1}{r}\left[\frac{X}{r}\right]_{nl}=0$$

$$i\omega(1-i\omega)\eta\beta_1\left[\frac{\partial U}{\partial r}\right]_{nl}+i\omega(1-i\omega)\eta\beta_2\left[\frac{U}{r}\right]_{nl}-N\omega(1-i\omega)\eta\beta_2\left[\frac{V}{r}\right]_{nl}$$
$$-k\omega(1-i\omega)\eta\beta_3[W]_{nl}+k\omega(1-i\omega)\eta P_3[X]_{nl} \quad (13a\sim e)$$
$$-k^2K_3Z+K_1\frac{\partial^2 Z}{\partial r^2}+K_2\left(-\frac{N^2}{r^2}Z+\frac{1}{r}\frac{\partial Z}{\partial r}\right)+i\omega(1-i\omega)\rho C_eY=0$$

The Legendre polynomial series are used to solve Eq. (13). Assuming the variables are expanded as the following form

$$\{U,\ V,\ W,\ X,\ Y\}=\sum_{m=0}^{\infty}Q_m(r)\left\{p_m^{(1)},\ p_m^{(2)},\ p_m^{(3)},\ p_m^{(4)},\ p_m^{(5)}\right\} \quad (14a)$$

Meanwhile, assuming

$$\frac{\partial Z}{\partial r}=H(r)\sum_{m=0}^{\infty}Q_m(r)p_m^{(6)} \quad (14b)$$

P_m is the Legendre polynomial of m-order. Eq. (14b) can achieve the isothermal boundary conditions. And

$$Q_m(r)=\sqrt{\frac{2m+1}{b-a}}P_m\left(\frac{2r-(a+b)}{b-a}\right) \quad (15)$$

Considering $Z=[Y]_{nl}$ and Eq. (14), it is

$$H(r)\sum_{m=0}^{\infty}Q_m(r)p_m^{(6)}=\sum_{m=0}^{\infty}p_m^{(5)}\frac{d}{dr}\int_0^h\alpha(|r-v|,\lambda)\sum_{m=0}^{\infty}Q_m(v)dv \quad (16)$$

It is noted that the solutions will be truncated at some M. Multiplying both ends of the equation by $Q_n(r)$ (n=0, 1, ..., M), then integration from a to b, one has

$$\boldsymbol{Gp}^{(6)}=\boldsymbol{Kp}^{(5)} \quad (17)$$

Here

$$\begin{cases}\boldsymbol{G}^{n,m}=\int_a^b Q_n(r)Q_m(r)dr\\ \boldsymbol{K}^{n,m}=\int_a^b Q_n(r)\frac{d}{dr}\int_0^h\alpha(|r-v|,\lambda)Q_m(v)dvdr\end{cases} \quad (18)$$

n, m are from 0 to M. Clearly, G is the unit matrix. Based on Eq. (18), the 6 unknowns are reduced to 5 unknowns, and the original problems can be solved.

Then, substituting Eq. (14) into Eq. (13), and multiplying both ends of the equation by $r^2Q_n(r)$ (n=0, 1, ..., M), integration from a to b, there is

$$k^2\begin{bmatrix}\boldsymbol{A}_{11}&\mathbf{0}&\mathbf{0}&\mathbf{0}&\mathbf{0}\\ \mathbf{0}&\boldsymbol{A}_{22}&\mathbf{0}&\mathbf{0}&\mathbf{0}\\ \mathbf{0}&\mathbf{0}&\boldsymbol{A}_{33}&\boldsymbol{A}_{34}&\mathbf{0}\\ \mathbf{0}&\mathbf{0}&\boldsymbol{A}_{43}&\boldsymbol{A}_{44}&\mathbf{0}\\ \mathbf{0}&\mathbf{0}&\mathbf{0}&\mathbf{0}&\boldsymbol{A}_{55}\end{bmatrix}\boldsymbol{p}+k\begin{bmatrix}\mathbf{0}&\mathbf{0}&\boldsymbol{B}_{13}&\boldsymbol{B}_{14}&\boldsymbol{B}_{15}\\ \mathbf{0}&\mathbf{0}&\boldsymbol{B}_{23}&\boldsymbol{B}_{24}&\mathbf{0}\\ \boldsymbol{B}_{31}&\boldsymbol{B}_{32}&\mathbf{0}&\mathbf{0}&\boldsymbol{B}_{35}\\ \boldsymbol{B}_{41}&\boldsymbol{B}_{42}&\mathbf{0}&\mathbf{0}&\mathbf{0}\\ \mathbf{0}&\mathbf{0}&\boldsymbol{B}_{53}&\boldsymbol{B}_{54}&\mathbf{0}\end{bmatrix}\boldsymbol{p}+\begin{bmatrix}\boldsymbol{D}_{11}&\boldsymbol{D}_{12}&\mathbf{0}&\mathbf{0}&\boldsymbol{D}_{15}\\ \boldsymbol{D}_{21}&\boldsymbol{D}_{22}&\mathbf{0}&\mathbf{0}&\boldsymbol{D}_{25}\\ \mathbf{0}&\mathbf{0}&\boldsymbol{D}_{33}&\boldsymbol{D}_{34}&\mathbf{0}\\ \mathbf{0}&\mathbf{0}&\boldsymbol{D}_{43}&\boldsymbol{D}_{44}&\boldsymbol{D}_{45}\\ \boldsymbol{D}_{51}&\boldsymbol{D}_{52}&\mathbf{0}&\mathbf{0}&\boldsymbol{D}_{55}\end{bmatrix}\boldsymbol{p}=\mathbf{0}$$

or $k^2Ap+kBp+Dp=0$ (19)

The dimension the all the submatrices (A_{ij}, B_{ij}, D_{ij}) is (M+1)×(M+1). The specific expressions can be found in the Appendix A.

Furthermore, Eq. (19) is transformed into a linear eigenvalue problem by using

$$\boldsymbol{q}=k\boldsymbol{p} \quad (20)$$

Coupling Eqs. (19) and (20), the complex dispersion (k-ω) can be obtained easily.

2.2. Electrical Closed-Circuit Condition

Considering the electrical closed-circuit condition, the Eq. (13d) would be modified to the following form

$$
\begin{aligned}
& ik\frac{\partial}{\partial r}\left(e_{15}\left[U\right]_{nl}\right)+ike_{31}\left[\frac{\partial U}{\partial r}\right]_{nl}+ike_{32}\left[\frac{U}{r}\right]_{nl}+ike_{15}\frac{1}{r}\left[U\right]_{nl}-kNe_{32}\left[\frac{V}{r}\right]_{nl}-kNe_{24}\frac{1}{r}\left[V\right]_{nl} \\
& -k^2e_{33}\left[W\right]_{nl}+\frac{\partial}{\partial r}\left(e_{15}\left[\frac{\partial W}{\partial r}\right]_{nl}\right)+e_{15}\frac{1}{r}\left[\frac{\partial W}{\partial r}\right]_{nl}-N^2e_{24}\frac{1}{r}\left[\frac{W}{r}\right]_{nl}+\frac{\partial P_3}{\partial r}Z+P_3\frac{\partial Z}{\partial r}+P_3\frac{Z}{r} \\
& +k^2\in_{33}\left[X\right]_{nl}-\frac{\partial}{\partial r}\left(\in_{11}\left[\frac{\partial X}{\partial r}\right]_{nl}\right)-\in_{11}\frac{1}{r}\left[\frac{\partial X}{\partial r}\right]_{nl}+N^2\in_{22}\frac{1}{r}\left[\frac{X}{r}\right]_{nl}=0
\end{aligned}
\tag{21}
$$

The other equations remain unchanged. The expanded form of the electrical potential is

$$X=\left(r-a\right)\left(r-b\right)\sum_{m=0}^{\infty}Q_m\left(r\right)p_m^{(5)} \tag{22}$$

Recombination equation, the complex dispersion (k-ω) can be obtained. The detailed process is shown in the Fig. 2.

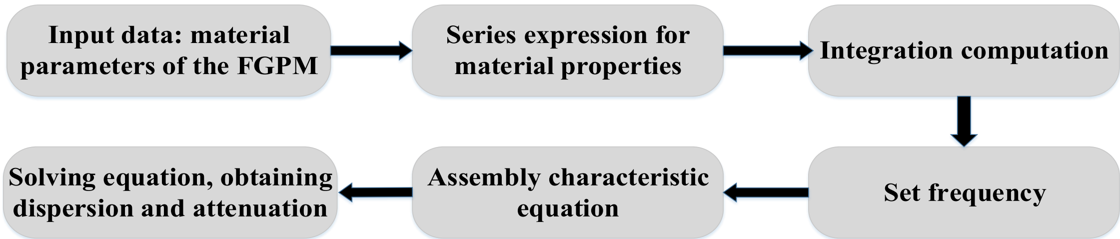

Figure 2. Schematic diagram of the solution process for the developed MNIE-LPSA

3. Integration Method

As Ref. [4, 32] shows, the integration by the command "int" in Matlab is much time-consuming. Thus, an iterative integration method is developed here to improve the computational efficiency. In Fig. 2, the integration computation will be implemented by the presented method in this section. Through analysis, all the integrals in this paper can be summarized in the following forms:

$$
\begin{cases}
G_1(n,m,j,p)=\int_{-1}^{1}\xi^jP_n(\xi)\dfrac{d^p}{d\xi^p}P_m(\xi)d\xi, \quad p=0,1,2;\ j=0,1,\ldots \\
G_2(n,m,j,p)=\int_{-1}^{1}\xi^jP_n(\xi)\dfrac{d^p}{d\xi^p}P_m(\xi)\dfrac{\partial H(\xi)}{\partial\xi}d\xi, \quad p=0,1;\ j=0,1,\ldots \\
G_3(n,m,j,p,k_1,k_2)=\int_{-1}^{1}\dfrac{\xi^j}{k_1\xi+k_2}P_n(\xi)\dfrac{d^p}{d\xi^p}P_m(\xi)\dfrac{\partial H(\xi)}{\partial\xi}d\xi, \quad p=0,1;\ j=0,1,\ldots \\
G_4(n,m,j,p,q,k_1,k_2)=\int_{-1}^{1}\dfrac{\xi^j}{(k_1\xi+k_2)^q}P_n(\xi)\dfrac{d^p}{d\xi^p}P_m(\xi)d\xi, \quad p=0,1;\ q=1,2;\ j=0,1,\ldots
\end{cases}
\tag{23}
$$

$$
\begin{cases}
H_1\left(m,p,\alpha,c,t,d\right)=\int_c^t e^{\alpha\xi}\xi^d\dfrac{d^p}{d\xi^p}P_m\left(\xi\right)d\xi, \\
H_2\left(m,p,\alpha,c,t,d,k_1,k_2\right)=\int_c^t e^{\alpha\xi}\xi^d\left(k_1\xi+k_2\right)^{-1}\dfrac{d^p}{d\xi^p}P_m\left(\xi\right)d\xi,
\end{cases}
\tag{24}
$$

$$
\begin{cases}
H_3\left(n,m,j,p,q,\alpha,c,t,d\right)=\int_{-1}^{1}t^jP_n\left(t\right)\dfrac{\partial^q}{\partial t^q}\int_c^t e^{\alpha(\xi-t)}\xi^d\dfrac{\partial^p}{\partial\xi^p}P_m\left(\xi\right)d\xi dt \\
H_4\left(n,m,j,p,q,\alpha,c,d,k_1,k_2\right)=\int_{-1}^{1}t^jP_n\left(t\right)\dfrac{\partial^q}{\partial t^q}\int_c^t e^{\alpha(\xi-t)}\xi^d\left(k_1\xi+k_2\right)^{-1}\dfrac{\partial^p}{\partial\xi^p}P_m\left(\xi\right)d\xi dt
\end{cases}
$$

$$p=0,\ 1;\ l=0,\ 1;\ q=0,\ 1;\ d=0,\ 1,\ 2. \tag{25}$$

$$\begin{cases} H_5\left(n,m,j,p,q,\alpha,c,d\right)=\int_{-1}^{1}t^jP_n\left(t\right)\frac{\partial H\left(t\right)}{\partial t}\frac{\partial^q}{\partial t^q}\int_c^t e^{\alpha(\xi-t)}\xi^d\frac{\partial^p}{\partial \xi^p}P_m\left(\xi\right)d\xi dt \\ H_6\left(n,m,j,p,q,\alpha,c,d,k_1,k_2\right)=\int_{-1}^{1}t^jP_n\left(t\right)\frac{\partial H\left(t\right)}{\partial t}\frac{\partial^q}{\partial t^q}\int_c^t e^{\alpha(\xi-t)}\xi^d\left(k_1\xi+k_2\right)^{-1}\frac{\partial^p}{\partial \xi^p}P_m\left(\xi\right)d\xi dt \end{cases}$$

p=0, 1; l=0, 1; q=0, 1; d=0, 1, 2. (26)

For the integrals G_j (j=1, 2), according to the analytical expressions by Yu et. al. [24], one has

$$G_1\left(n,m,p,j\right)=\sum_{s=0}^{\left\lfloor\frac{m}{2}\right\rfloor}\left(-1\right)^s\frac{\left(2m-2s\right)!}{2^m s!(m-s)!(m-2s-p)!}I_1\left(j+m-2s-p,n\right) \tag{27}$$

$$\begin{cases} G_2\left(n,m,0,j\right)=(-1)^{j+n+m}-1 \\ G_2\left(n,m,1,j\right)=(-1)^{j+m+1}P_n\left(-1\right)\frac{\Gamma\left(m+2\right)}{2\Gamma\left(m\right)}-P_n\left(1\right)\frac{\Gamma\left(m+2\right)}{2\Gamma\left(m\right)} \end{cases} \tag{28}$$

Here the series of Legendre polynomial $P_m(t)$ are used [39, 40],

$$P_m\left(t\right)=\sum_{s=0}^{\left\lfloor\frac{m}{2}\right\rfloor}\left(-1\right)^s\frac{\left(2m-2s\right)!}{2^m s!(m-s)!(m-2s)!}t^{m-2s} \tag{29}$$

For the integral G_3, it is

$$G_3\left(n,m,j,p,k_1,k_2\right)=(-1)^{j+m+1}P_n\left(-1\right)\frac{\Gamma\left(m+2\right)}{2\Gamma\left(m\right)}\frac{1}{-k_1+k_2}-P_n\left(1\right)\frac{\Gamma\left(m+2\right)}{2\Gamma\left(m\right)}\frac{1}{k_1+k_2} \tag{30}$$

The G_4 will be evaluated based on the following results. Then for the integrals H_j (j=1, 2, 3, 4, 5, 6), the following integrals should be given first,

$$\begin{cases} I_1\left(j,n\right)=\int_{-1}^{1}\xi^jP_n\left(\xi\right)d\xi, \\ I_2\left(j,\alpha,c,d\right)=\int_c^d e^{\alpha\xi}\xi^jd\xi, \\ I_3\left(j,\alpha,c,d,k_1,k_2\right)=\int_c^d e^{\alpha\xi}\xi^j\left(k_1\xi+k_2\right)^{-1}d\xi, \end{cases}$$

$$\begin{cases} I_4\left(n,m,\alpha,c\right)=\int_{-1}^{1}t^n\int_c^t e^{\alpha(\xi-t)}\xi^m d\xi dt \\ I_5\left(j,p,k_1,k_1\right)=\int_{-1}^{1}\xi^j\left(k_1\xi+k_2\right)^{-p}d\xi, \quad p=1,2 \\ I_6\left(n,m,\alpha,c,k_1,k_2\right)=\int_{-1}^{1}t^n\int_c^t e^{\alpha(\xi-t)}\left(k_1\xi+k_2\right)^{-1}\xi^m d\xi dt \end{cases} \tag{31a-b}$$

For I_1, it is easy to get the following expression based on the orthogonality of Legendre polynomials [40, p160],

$$I_1\left(j,n\right)=\int_{-1}^{1}t^jP_n\left(t\right)dt=\begin{cases} 0, \quad j<n \\ 0, \quad j>n, \quad \mathrm{mod}(j-n,2)=1 \\ 2^{n+1}\dfrac{j!\left(\dfrac{j+n}{2}\right)!}{\left(\dfrac{j-n}{2}\right)!\left(j+n+1\right)!}, \quad j>n, \quad \mathrm{mod}(j-n,2)=0 \end{cases} \tag{32}$$

For I_2 and I_3, one has

$$\begin{cases} I_2(0,\alpha,c,d) = \frac{1}{\alpha}\left(e^{\alpha d} - e^{\alpha c}\right) \\ I_2(j,\alpha,c,d) = \frac{1}{\alpha}\left(d^j e^{\alpha d} - c^j e^{\alpha c}\right) - \frac{j}{\alpha} I_2(j-1,\alpha,c,d) \end{cases} \tag{33}$$

and

$$\begin{cases} I_3(0,c,d,k_1,k_2) = \int_c^d e^{\alpha t}\left(k_1 t + k_2\right)^{-1} dt = \frac{1}{k_1} e^{-\frac{\alpha k_2}{k_1}} \left[\mathrm{Ei}\left(\frac{\alpha}{k_1}(k_1 d + k_2)\right) - \mathrm{Ei}\left(\frac{\alpha}{k_1}(k_1 c + k_2)\right)\right] \\ I_3(j,\alpha,c,d,k_1,k_2) = \frac{1}{k_1} I_2(j-1,\alpha,c,d) - \frac{k_2}{k_1} I_3(j-1,1,\alpha,c,d,k_1,k_2) \end{cases} \tag{34}$$

Ei is the exponential integral function given as [39, 40]

$$\mathrm{Ei}(x) = \int_{-\infty}^{x} \frac{e^t}{t} dt \tag{35}$$

For I_4, it is easy to have

$$\begin{aligned} I_4(0,m,\alpha,c) &= -\frac{1}{\alpha}\left[e^{-\alpha t} \int_c^t e^{\alpha\xi} \xi^m d\xi \right]_{-1}^{1} + \frac{1}{\alpha} \int_{-1}^{1} e^{-\alpha t} d\left[\int_c^t e^{\alpha\xi}\xi^m d\xi \right] \\ &= -\frac{1}{\alpha}\left[e^{-\alpha t} I_2(m,\alpha,c,t)\right]_{-1}^{1} + \frac{1}{\alpha(m+1)}\left(1-(-1)^{m+1}\right) \end{aligned} \tag{36}$$

$$\begin{aligned} & I_4(n,m,\alpha,c) = \int_{-1}^{1} t^n e^{-\alpha t} \int_c^t e^{\alpha\xi}\xi^m d\xi dt \\ & = -\frac{1}{\alpha}\left[t^n e^{-\alpha t} \int_c^t e^{\alpha\xi}\xi^m d\xi \right]_{-1}^{1} + \frac{1}{\alpha}\int_{-1}^{1} e^{-\alpha t} d\left[t^n \int_c^t e^{\alpha\xi}\xi^m d\xi\right] \\ & = -\frac{1}{\alpha}\left[t^n e^{-\alpha t} I_2(m,\alpha,c,t)\right]_{-1}^{1} + \frac{1}{\alpha(n+m+1)}\left(1-(-1)^{n+m+1}\right) + \frac{n}{\alpha} I_4(n-1,m,\alpha,c) \end{aligned} \tag{37}$$

For I_5, one has

$$\begin{cases} I_5(0,1,k_1,k_2) = \frac{1}{k_1}\left[\ln(k_1+k_2) - \ln(-k_1+k_2)\right] \\ I_5(j,1,k_1,k_2) = \frac{1}{jk_1}\left[1-(-1)^j\right] - \frac{k_2}{k_1} I_5(j-1,1,k_1,k_2) \end{cases} \tag{38}$$

$$\begin{cases} I_5(0,2,k_1,k_2) = -\frac{1}{k_1}\left(\frac{1}{k_1+k_2} - \frac{1}{-k_1+k_2}\right) \\ I_5(j,2,k_1,k_2) = \frac{1}{k_1} I_5(j-1,1) - \frac{k_2}{k_1} I_5(j-1,2) \end{cases} \tag{39}$$

For I_6, the integral expression can be obtained as

$$\begin{aligned} & I_6(0,m,\alpha,c,k_1,k_2) = \int_{-1}^{1} e^{-\alpha t}\int_c^t e^{\alpha\xi}(k_1\xi+k_2)^{-1}\xi^m d\xi dt \\ & = -\frac{1}{\alpha}\left[e^{-\alpha t}\int_c^t e^{\alpha\xi}(k_1\xi+k_2)^{-1}\xi^m d\xi\right]_{-1}^{1} + \frac{1}{\alpha}\int_{-1}^{1} e^{-\alpha t} d\left[\int_c^t e^{\alpha\xi}(k_1\xi+k_2)^{-1}\xi^m d\xi\right] \\ & = -\frac{1}{\alpha}\left[e^{-\alpha t} I_3(m,\alpha,c,t,k_1,k_2)\right]_{-1}^{1} + \frac{1}{\alpha} I_5(m,1,k_1,k_2) \end{aligned} \tag{40}$$

$$\begin{aligned} & I_6(n,m,\alpha,c,k_1,k_2) = \int_{-1}^{1} t^n e^{-\alpha t}\int_c^t e^{\alpha\xi}(k_1\xi+k_2)^{-1}\xi^m d\xi dt \\ & = -\frac{1}{\alpha}\left[t^n e^{-\alpha t}\int_c^t e^{\alpha\xi}(k_1\xi+k_2)^{-1}\xi^m d\xi\right]_{-1}^{1} + \frac{1}{\alpha}\int_{-1}^{1} e^{-\alpha t} d\left[t^n\int_c^t e^{\alpha\xi}(k_1\xi+k_2)^{-1}\xi^m d\xi\right] \\ & = -\frac{1}{\alpha}\left[t^n e^{-\alpha t} I_3(m,\alpha,c,t,)\right]_{-1}^{1} + \frac{1}{\alpha} I_5(n+m,1,k_1,k_2) + \frac{n}{\alpha} I_6(n-1,m,\alpha,c,k_1,k_2) \end{aligned} \tag{41}$$

Then in view of the above integrals, one has

$$G_4\left(n,m,j,p,k_1,k_2\right)=\sum_{s=0}^{\left\lfloor \frac{n}{2}\right\rfloor}(-1)^s\frac{(2n-2s)!}{2^n s!(n-s)!(n-2s)!}\sum_{l=0}^{\left\lfloor \frac{m-p}{2}\right\rfloor}(-1)^l\frac{(2m-2l)!}{2^m l!(m-l)!(m-2l-p)!}\times I_5\left(j+n+m-2s-2l-p,2\right) \tag{42}$$

$$\begin{aligned} H_1\left(m,p,\alpha,c,t,d\right)&=\int_c^t e^{\alpha\xi}\xi^d\frac{d^p}{d\xi^p}P_m(\xi)d\xi \\ &=\sum_{s=0}^{\left\lfloor \frac{m}{2}\right\rfloor}(-1)^s\frac{(2m-2s)!}{2^m s!(m-s)!(m-2s-p)!}\int_c^t e^{\alpha\xi}\xi^{m+d-2s-p}d\xi \\ &=\sum_{s=0}^{\left\lfloor \frac{m}{2}\right\rfloor}(-1)^s\frac{(2m-2s)!}{2^m s!(m-s)!(m-2s-p)!}I_2\left(m+d-2s-p,\alpha,c,t\right) \end{aligned} \tag{43}$$

$$\begin{aligned} H_2\left(m,p,\alpha,c,t,d,k_1,k_2\right)&=\int_c^t e^{\alpha\xi}\xi^d\left(k_1\xi+k_2\right)^{-1}\frac{d^p}{d\xi^p}P_m(\xi)d\xi \\ &=\sum_{s=0}^{\left\lfloor \frac{m}{2}\right\rfloor}(-1)^s\frac{(2m-2s)!}{2^m s!(m-s)!(m-2s-p)!}I_3\left(m+d-2s-p,\alpha,c,t,k_1,k_2\right) \end{aligned} \tag{44}$$

For H_j(j=3, 4, 5, 6), the expressions will be given by considering different q. When q=0, they are

$$\begin{aligned} H_3\left(n,m,j,p,0,\alpha,c,t,d\right)&=\int_{-1}^1 t^jP_n(t)\int_c^t e^{\alpha(\xi-t)}\xi^d\frac{\partial^p}{\partial\xi^p}P_m(\xi)d\xi dt \\ &=\sum_{s=0}^{\left\lfloor \frac{n}{2}\right\rfloor}(-1)^s\frac{(2n-2s)!}{2^n s!(n-s)!(n-2s)!}\sum_{l=0}^{\left\lfloor \frac{m-p}{2}\right\rfloor}(-1)^l\frac{(2m-2l)!}{2^m l!(m-l)!(m-2l-p)!}I_4\left(j+n-2s,m+d-2l-p,\alpha,c\right) \end{aligned} \tag{45}$$

$$\begin{aligned} H_4\left(n,m,j,p,0,\alpha,c,d,k_1,k_2\right)&=\int_{-1}^1 t^jP_n(t)\int_c^t e^{\alpha(\xi-t)}\xi^d\left(k_1\xi+k_2\right)^{-1}\frac{\partial^p}{\partial\xi^p}P_m(\xi)d\xi dt \\ &=\sum_{s=0}^{\left\lfloor \frac{n}{2}\right\rfloor}(-1)^s\frac{(2n-2s)!}{2^n s!(n-s)!(n-2s)!}\sum_{l=0}^{\left\lfloor \frac{m-p}{2}\right\rfloor}(-1)^l\frac{(2m-2l)!}{2^m l!(m-l)!(m-2l-p)!}I_6\left(j+n-2s,m+d-2l-p,\alpha,c,k_1,k_2\right) \end{aligned} \tag{46}$$

$$\begin{aligned} H_5\left(n,m,j,p,0,\alpha,c,d\right)&=(-1)^{j+n}\left[\sum_{s=0}^{\left\lfloor \frac{m}{2}\right\rfloor}(-1)^s\frac{(2m-2s)!}{2^m s!(m-s)!(m-2s-p)!}e^{\alpha}I_2\left(m+d-2s-p,\alpha,c,-1\right)\right]_{t=-1} \\ &-\left[\sum_{s=0}^{\left\lfloor \frac{m-p}{2}\right\rfloor}(-1)^s\frac{(2m-2s)!}{2^m s!(m-s)!(m-2s-p)!}e^{-\alpha}I_2\left(m+d-2s-p,\alpha,c,1\right)\right]_{t=1} \end{aligned} \tag{47}$$

$$\begin{aligned} H_6\left(n,m,j,p,0,\alpha,c,d,k_1,k_2\right)&=(-1)^{j+n}\left[\sum_{s=0}^{\left\lfloor \frac{m}{2}\right\rfloor}(-1)^s\frac{(2m-2s)!}{2^m s!(m-s)!(m-2s-p)!}e^{\alpha}I_3\left(m+d-2s-p,\alpha,c,-1,k_1,k_2\right)\right] \\ &-\left[\sum_{s=0}^{\left\lfloor \frac{m-p}{2}\right\rfloor}(-1)^s\frac{(2m-2s)!}{2^m s!(m-s)!(m-2s-p)!}e^{-\alpha}I_3\left(m+d-2s-p,\alpha,c,1,k_1,k_2\right)\right] \end{aligned} \tag{48}$$

When q=1, one has

$$H_3\left(n,m,j,p,1,\alpha,c,t,d\right)=-\alpha H_3\left(n,m,j,p,0,\alpha,c,t,d\right)+G_1\left(n,m,j+d,p\right) \tag{49}$$

$$H_4\left(n,m,j,p,1,\alpha,c,d,k_1,k_2\right)=-\alpha H_4\left(n,m,j,p,0,\alpha,c,d,k_1,k_2\right)+G_4(n,m,j+d,p,1) \tag{50}$$

$$H_5\left(n,m,j,p,1,\alpha,c,d\right)=$$
$$-\alpha\left\{\begin{array}{l}(-1)^{j+n}\left[\sum_{s=0}^{\left\lfloor\frac{m-p}{2}\right\rfloor}(-1)^s\dfrac{(2m-2s)!}{2^m s!(m-s)!(m-2s-p)!}e^{\alpha}I_2\left(m+d-2s-p,\alpha,c,-1\right)\right]_{t=-1}\\-\left[\sum_{s=0}^{\left\lfloor\frac{m-p}{2}\right\rfloor}(-1)^s\dfrac{(2m-2s)!}{2^m s!(m-s)!(m-2s-p)!}e^{-\alpha}I_2\left(m+d-2s-p,\alpha,c,1\right)\right]_{t=1}\end{array}\right\}+G_2\left(n,m,j+d,1\right) \tag{51}$$

$$H_6\left(n,m,j,p,1,\alpha,c,d,k_1,k_2\right)=-\alpha H_6\left(n,m,j,p,0,\alpha,c,d,k_1,k_2\right)+G_3\left(n,m,j+d,1,k_1,k_2\right) \tag{52}$$

When q=2, H_3 and H_4 also have

$$\begin{aligned}H_3\left(n,m,j,p,2,\alpha,c,t,d\right)&=\alpha^2H_3\left(n,m,j,p,0,\alpha,c,t,d\right)-\alpha G_1\left(n,m,j+d,p\right)\\&\quad+G_1\left(n,m,j+d,p+1\right)+dG_1\left(n,m,j+d-1,p\right)\end{aligned} \tag{53}$$

$$\begin{aligned}H_4\left(n,m,j,p,2,\alpha,c,d,k_1,k_2\right)&=\alpha^2H_4\left(n,m,j,p,0,\alpha,c,d,k_1,k_2\right)-\alpha G_4\left(n,m,j+d,p,1\right)\\&\quad+G_4\left(n,m,j+d,p+1,1\right)-k_1G_4\left(n,m,j+d,p,2\right)+dG_4\left(n,m,j+d-1,p,1\right)\end{aligned} \tag{54}$$

The derivation of all integral solving formulas has been completed. Based on the above integration formula, efficient analysis of guided wave characteristics in nano hollow cylinders can be achieved.

4. Algorithm Analysis

In this section, numerical results are presented and discussed for thermoelastic waves in FGPM nano hollow cylinders. The k=Re(k)+Im(k)*i is the nondimensional wave number. Re(k) and Im(k) denote propagation and attenuation, respectively.

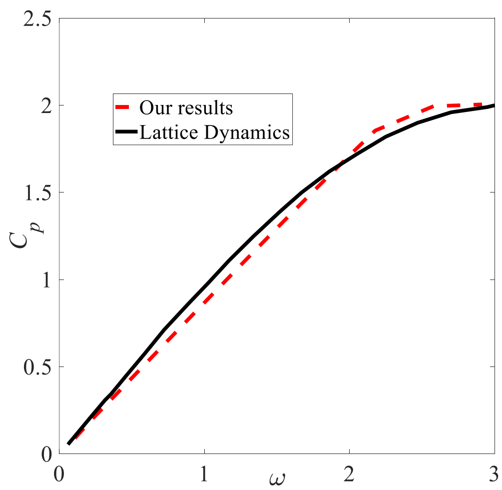

Figure 3. Comparing our results with those from Lattice Dynamics [41], λ=0.28

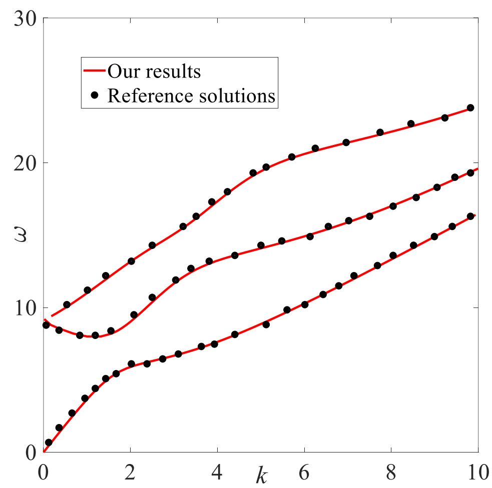

Figure 4. Comparing our results with the exact solutions [42], λ=1E-3

4.1. Numerical Verification

The conventional LPSA for FGM structures has been proved in many references [31, 32], and the existing works lack wave solutions from the nonlocal integral elasticity. Thus, the verification will be implemented in two aspects: (1) comparison with the results from Lattice Dynamics for carbon nanotubes; (2) comparison with the results from electric-elastic coupling waves for classical hollow cylinder.

The comparison for the wave in a carbon nanotube [41] is shown in Fig. 3. The elastic modulus E=1.1TPa. The poisson's ratio ν=0.2. The density ρ=2236Kg/m^3. The nonlocal parameter λ=0.28. Obviously, the two results from the LPSA and the Lattice Dynamics are closed, which demonstrates the effectiveness of the presented MNIE-LPSA for the nanostructures. Another comparison for the coupled electric-elastic waves is depicted in Fig. 4. The material properties can be seen in Table 1. The nonlocal parameter λ=0.001. The first three modes in Fig. 2(b) in Ref. [42] are selected for comparison. Clearly, the two results are consistent, which demonstrates that the presented MNIE-LPSA is valid for the coupled wave. These examples indicate the correctness of the proposed method.

Table 1. Material properties in Ref. [42]

Property	C_{11}	C_{12}	C_{13}	C_{33}	C_{44}	ρ
PZT-5H	126	79.5	84.1	117	25.6	7600
	ε_{11}	ε_{33}	e_{31}	e_{33}	e_{15}	
PZT-5H	15	13	-6.5	23.3	17	

Units: $C_{ij}(10^9 N\cdot m^{-2})$, $e_{ij}(C\cdot m^{-2})$, $\varepsilon_{ij}(10^{-9}C^2\cdot N^{-1}\cdot m^{-2})$, $\rho(10^3 kg\cdot m^{-3})$

Table 2. Material properties [43]

Property	C_{11}	C_{12}	C_{13}	C_{33}	C_{55}	e_{31}	e_{33}	e_{15}	ρ
CdSe	74.1	45.2	39.3	83.6	13.2	-0.16	0.347	-0.138	5.504
PZT-5A	139	77.8	75.4	113	25.6	-6.98	13.8	13.4	7.75
	ε_{11}	ε_{33}	K_1	K_3	β_1	β_3	P_1	P_3	C_e
CdSe	8.26	9.03	9	9	0.621	0.551	-2.94	-2.94	260
PZT-5A	600	547	1.5	1.5	1.52	1.53	-452	-452	420

Units: $C_{ij}(10^9 N\cdot m^{-2})$, $e_{ij}(C\cdot m^{-2})$, $\varepsilon_{ij}(10^{-11}C^2\cdot N^{-1}\cdot m^{-2})$, $K_i(W\cdot m^{-1}\cdot K^{-1})$, $\beta_i(10^6 N\cdot K^{-1}\cdot m^{-2})$, $P_i(10^{-6}C\cdot K^{-1}\cdot m^{-2})$, $C_e(J\cdot kg^{-1}\cdot K^{-1})$, $\rho(10^3 kg\cdot m^{-3})$

4.2. Computational Efficiency

Computational efficiency is an important indicator of numerical algorithm performance. With the help of the material parameters in Table 2, this section evaluates the computational efficiency of the proposed integration method and the “int” command in Matlab. The total CPU time for the wave analysis mainly contains the integral calculation time and eigenvalue calculation time. For expanded order M≤5, the eigenvalue calculation time for one frequency is less than 0.1s. Therefore, only the integral calculation time is considered in Table 3. Due to excessive time consumption by using the “int” command in Matlab, no information was provided for M=4 and 5. Besides, the integration by using the “int” command consumes very much CPU time, and the CPU time increases rapidly as the gradient index or the expanded order increases. However, the presented method only consumes several seconds for the integrals with M from 1 to 5. The computational efficiency can be improved by 99%. This example demonstrates the significant advantage of the proposed method in CPU time.

Table 3. CPU time for FGM hollow cylinders using MNIE-LPSA (s)

M		1	2	3	4	5
L=1	Presented	0.20	0.38	0.67	1.17	2.08
	“int” command	1548.1	2791.9	4034.7	-	-
L=2	Presented	0.28	0.52	0.89	1.53	2.66
	“int” command	7512.7	11737.0	16527.0	-	-
L=3	Presented	0.38	0.67	1.16	1.91	3.31
	“int” command	23335.0	35747.0	48725.0	-	

5. Numerical Analysis

In this section, the nonlocal effect, piezoelectric effect, gradient index (L), radius to thickness ratio (μ), and circumferential order (N) on the thermoelastic wave characteristics are investigated. The material parameters are shown in Table 2. The thermoelastic coupling coefficient η=1.5E-3. Without explanation, the inner radius a=4, and the outer radius b=5. The gradient index L=1.

5.1. Nonlocal Effect

The nonlocal effect on wave behaviors of axisymmetric modes (N=0) is analyzed in Figs. 5-7. There are significant differences in the results of the phase velocity and attenuation with the different nonlocal parameters (λ). This indicates the necessity of considering the nonlocal effect on the wave propagation in nanostructures. Fig. 5 depicts the phase velocity and attenuation curves of the first thermal wave. Clearly, with the nonlocal parameter enlarging, the phase velocity decreases, and the attenuation increases. Meanwhile, the ratios of the attenuation coefficient Im(k) are larger than those of the phase velocity C_p. This indicates that the nonlocal effect on attenuation is more significant than that on phase velocity. The ratios are defined as

$$\begin{cases} Rv1=\dfrac{C_p^{\lambda=0.02}-C_p^{\lambda=0.06}}{C_p^{\lambda=0.02}} \\ Rv2=\dfrac{C_p^{\lambda=0.02}-C_p^{\lambda=0.1}}{C_p^{\lambda=0.02}} \end{cases} \text{and} \begin{cases} Rk1=\dfrac{\mathrm{Im}(k^{\lambda=0.06})-\mathrm{Im}(k^{\lambda=0.02})}{\mathrm{Im}(k^{\lambda=0.02})} \\ Rk2=\dfrac{\mathrm{Im}(k^{\lambda=0.1})-\mathrm{Im}(k^{\lambda=0.02})}{\mathrm{Im}(k^{\lambda=0.02})} \end{cases} \tag{55}$$

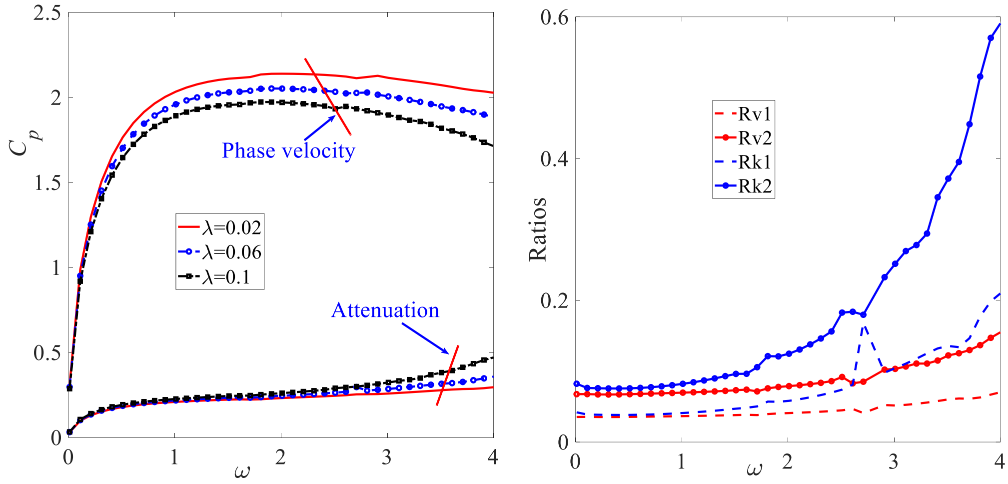

(a) (b)

Figure 5. Phase velocity and attenuation curves of the first thermal wave

Figs. 6 and 7 give the phase velocity and attenuation curves of the first four longitudinal waves and the first two torsional waves, respectively. For N=0, no attenuation appears in the torsional waves. With the nonlocal parameter enlarging, it is evident that all the phase velocities decrease in Fig. 7. Actually, the decrease of phase velocity is due to the softening effect of nonlocal parameters on nanostructures. The cut-off frequencies of the 3rd and 4th modes of the longitudinal waves, and the 2nd mode of the torsional wave decreases clearly as the nonlocal parameter increases. This implies that the cut-off frequencies are sensitive to the nonlocal parameter. Simultaneously, the decrease of the cut-off frequency means an increase in the wave propagation frequency domain. In Fig. 6(b), the attenuation of the higher-order modes is larger than that of the lower-order modes. From the perspective of energy dissipation, wave-based devices should prioritize the selection of lower-order modes.

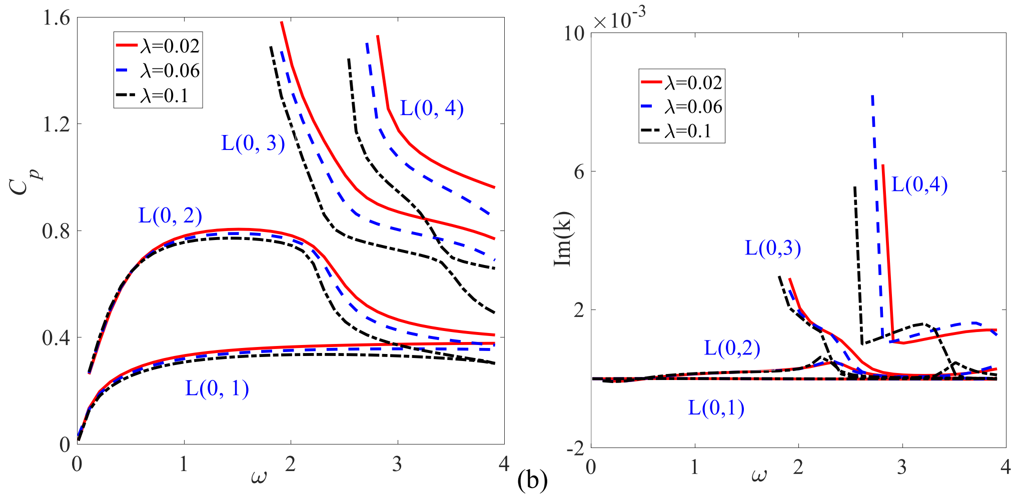

(a) Phase velocity (b) Attenuation

Figure 6. Nonlocal effect on the first four longitudinal waves

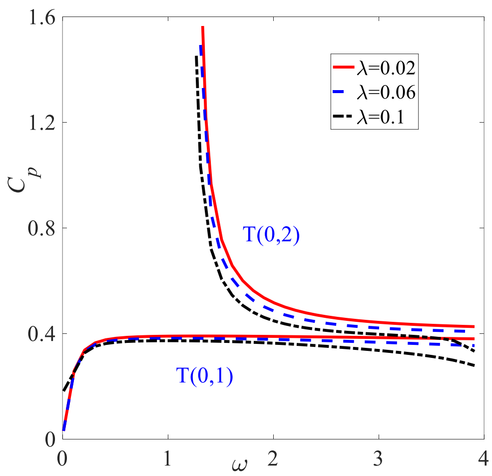

Figure 7. Nonlocal effect on the phase velocity of first two torsional waves

For the 3rd and 4th modes, Fig. 6(b) declares that the attenuation almost decreases as the nonlocal parameter increases. As shown in Fig.8, the nonlocal effect on attenuation is more significant than that on phase velocity, which is similar to the thermal wave. Fig.8(a) also indicates that the nonlocal effect is enhanced with increasing modal order. The nonlocal effect on the attenuation of the higher modes is more obvious, which is the same as that on phase velocity. This example states that the design of the wave-based nanodevices must consider the nonlocal effect, especially for its attenuation.

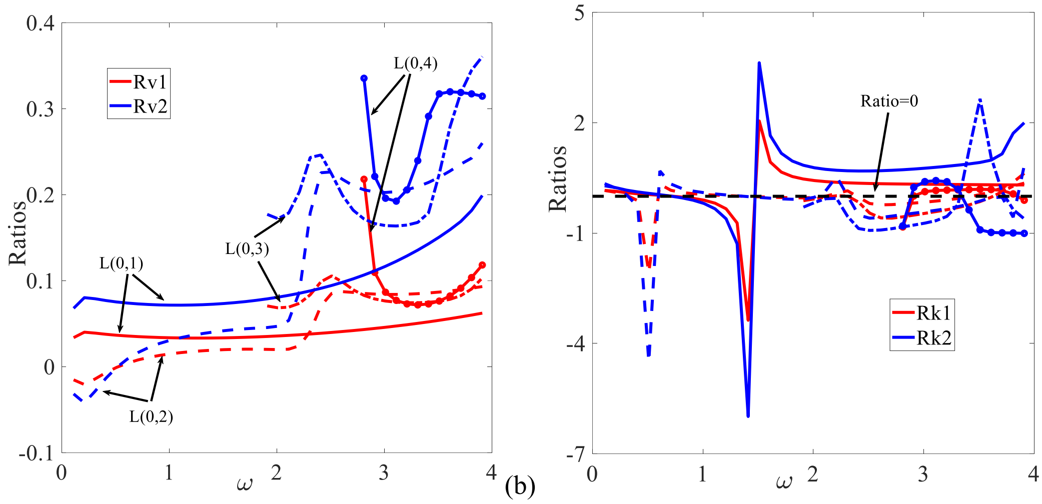

(a) Phase velocity (b) Attenuation

Figure 8. Ratios of the phase velocity and attenuation of the first four longitudinal waves

5.2. Circumferential Order

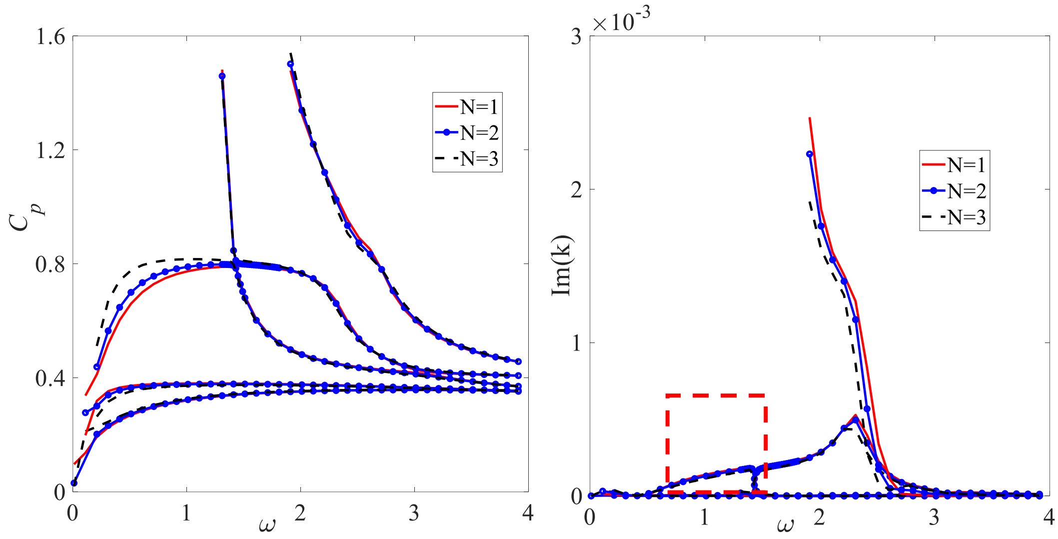

(a) Phase velocity (b) Attenuation

Figure 9. Phase velocity and attenuation of the first five flexural waves

Fig. 9 shows the variation of the phase velocity and attenuation along with circumferential order N. λ=0.06. Only the phase velocities and attenuation at low frequencies change clearly, which is consistent with the published results [44]. The attenuation has a sharp change in the red box in Fig. 9(b). The reason is that: for the 3rd and 4th flexural waves, the modal exchange appears near ω=1.44. Thus, the modal exchange causes the attenuation of the 3rd mode decrease drastically, and that of the 4th mode increase drastically, as shown in Fig. 10.

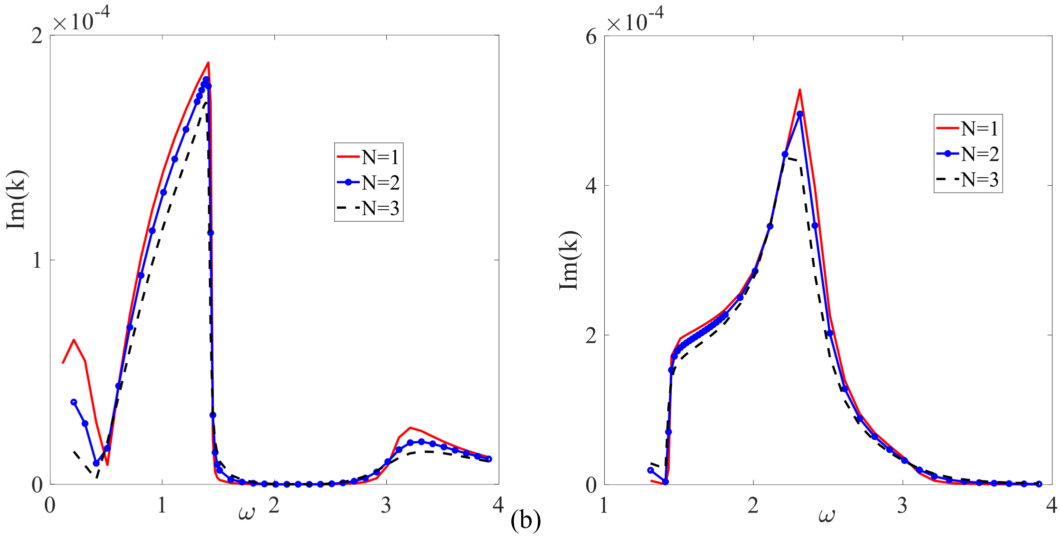

(a) 3[rd] flexural waves (b) 4[th] flexural waves

Figure 10. Attenuation of the 3[rd] and 4[th] flexural waves

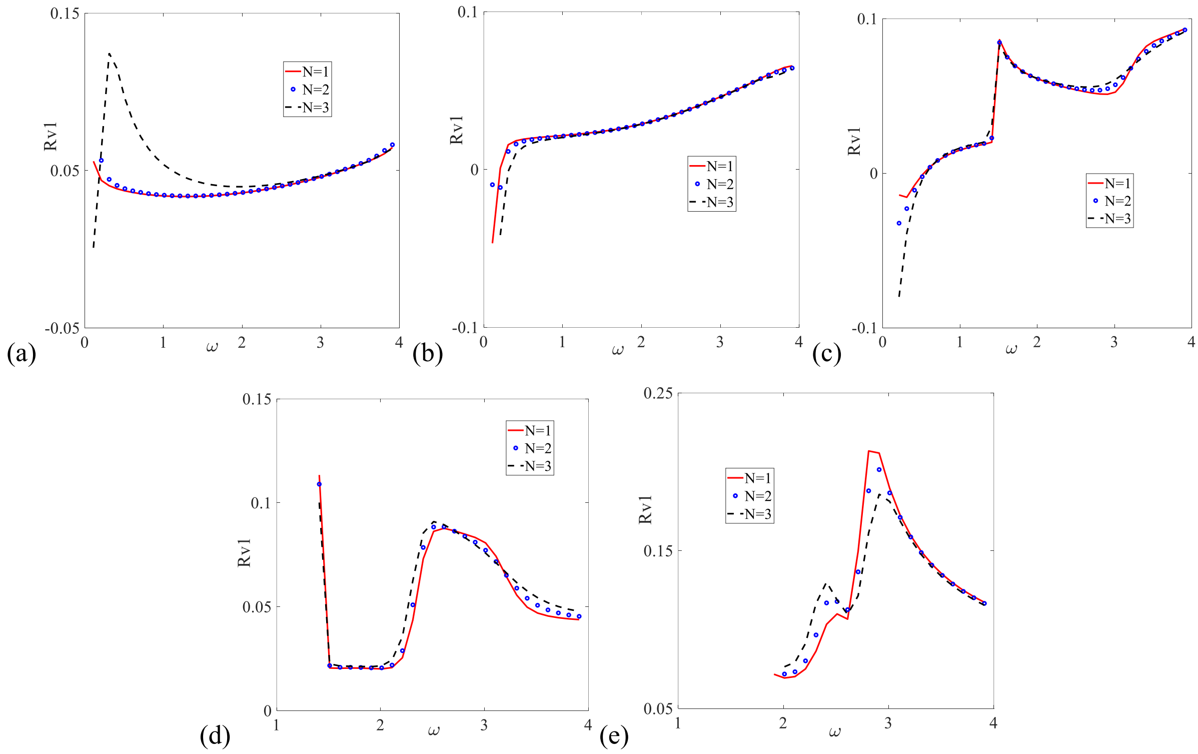

Figure 11. Rv1 of the first five modes with different N, (a)-(e) are the 1[st] to 5[th] modes

Fig. 11 shows the intensity of nonlocal effects with different circumferential orders. The phase velocity with λ=0.02 is compared. Obviously, the nonlocal effect on phase velocity with different circumferential orders is more pronounced at low frequencies. The larger the circumferential order or the mode order, the more pronounced the nonlocal effect. Meanwhile, the first three modes (without cut-off frequency) all exhibit strengthening effects at low frequencies, while high-order modes (4-5th order modes) with cut-off frequencies do not exhibit strengthening effects. This phenomenon has never been seen before from the nonlocal differential elasticity. This indicates that for wave propagation, the nonlocal effect may not necessarily be entirely softening effect, especially at low frequency and lower-mode. Simultaneously, for a fixed mode, the nonlocal effect will increase first and then decrease with the increase of frequency. Research can provide a theoretical basis for the selection of the circumferential order and frequency in wave-based nanodevices.

5.3. Radius to Thickness Ratio

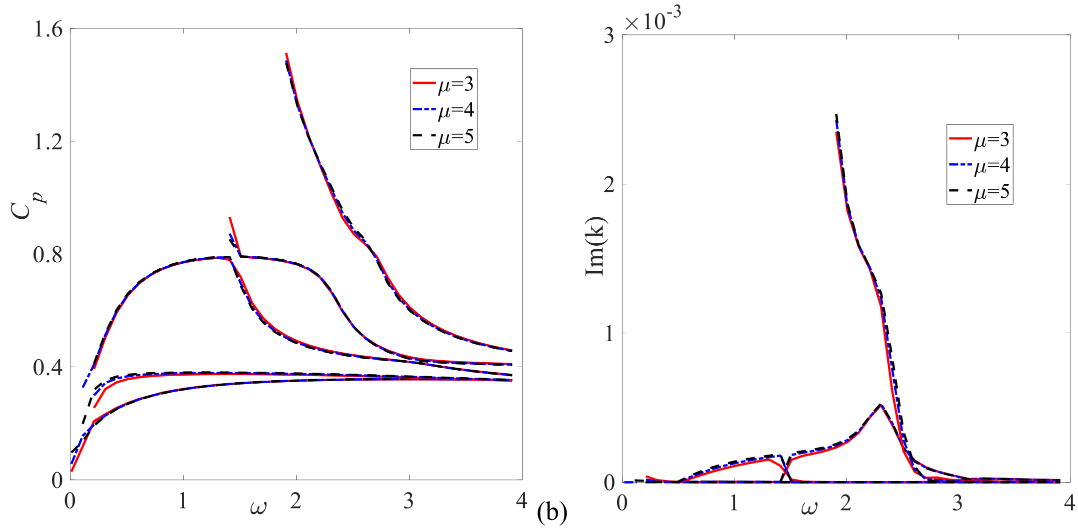

(a) Phase velocity (b) Attenuation

Figure 12. Phase velocity and attenuation of the first five flexural waves with different μ

The effect of the radius to thickness ratio μ on the phase velocity and attenuation of the first five flexural waves is considered in Fig. 12. Evidently, the phase velocity is mainly affected at low frequencies and near cut-off frequencies. The phase velocity and attenuation decrease as μ increases. This is consistent with existing research findings. Besides, the effects of radius to thickness ratio μ and the nonlocal parameter λ on cut-off frequencies are displayed in Table 4. Table 4 shows that the cut-off frequency decreases with increasing λ or μ. This implies that the effect of μ and λ on the cut-off frequency is mutually reinforcing. The results of the Rv1 and Rv2 indicate that the nonlocal effects on cut-off frequencies with different μ are closed.

Table 4. Cut-off frequencies of the 4th and 5th modes

	μ=2		μ=3		μ=4		μ=5	
	4th one	5th one	4th one	5th one	4th one	5th one	4th one	5th one
λ=0.02	1.423	1.634	1.319	1.584	1.298	1.575	1.29	1.573
λ=0.06	1.399	1.619	1.300	1.573	1.279	1.563	1.271	1.561
λ=0.1	1.357	1.580	1.263	1.535	1.243	1.527	1.235	1.525
Rv1	0.017	0.0092	0.014	0.0069	0.015	0.0076	0.015	0.0076
Rv2	0.046	0.033	0.042	0.031	0.042	0.030	0.043	0.031

5.4. Gradient Index

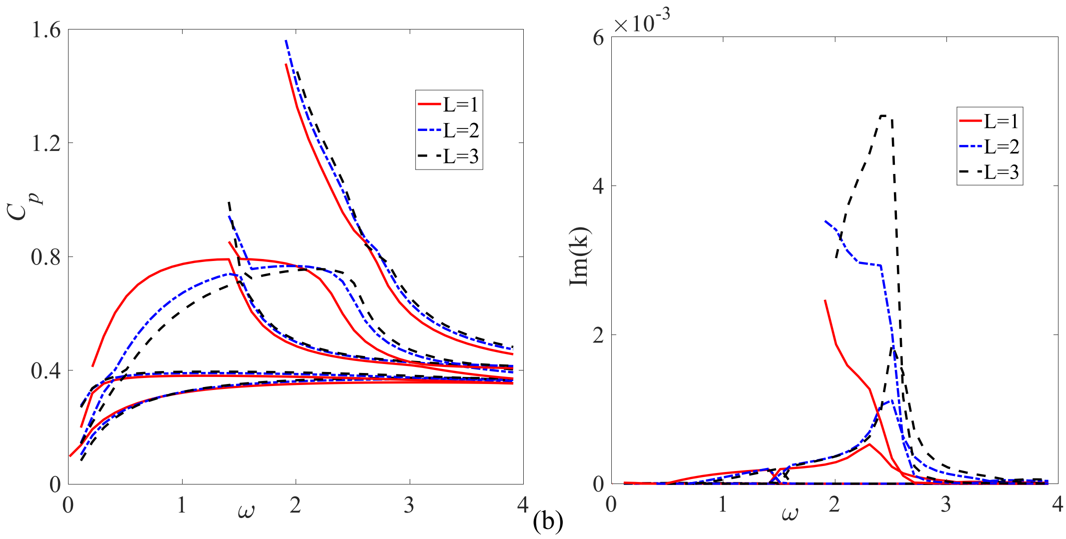

(a) Phase velocity (b) Attenuation

Figure 13. Phase velocity and attenuation of the first five flexural waves with different L

Fig. 13 shows the effect of the gradient index L on the phase velocity and attenuation of the first five flexural waves. The phase velocity and attenuation both are affected evidently by L. The phase velocity increases with the increasing L, except for the 1st and 3rd modes at low frequencies. However, the influence of gradient index on attenuation is complex. Meanwhile, the reinforcement effect of the nonlocal elasticity also appears in the 1st to 3rd modes at low frequencies. Fig.14

displays the intensity of nonlocal effects with different L. The Rv1 of the 1st and 2nd modes only are distinctive at low frequencies. For the lower-order modes, the intensities of nonlocal effects with different L only are different at low frequencies, but are closed at high frequencies. For the 3rd to 5th modes, the intensities of nonlocal effects with different L are different for all frequencies. Thus, by simultaneously adjusting the gradient index and nonlocal parameters, different phase velocities and attenuation can be designed to meet the specific requirements of wave-based devices.

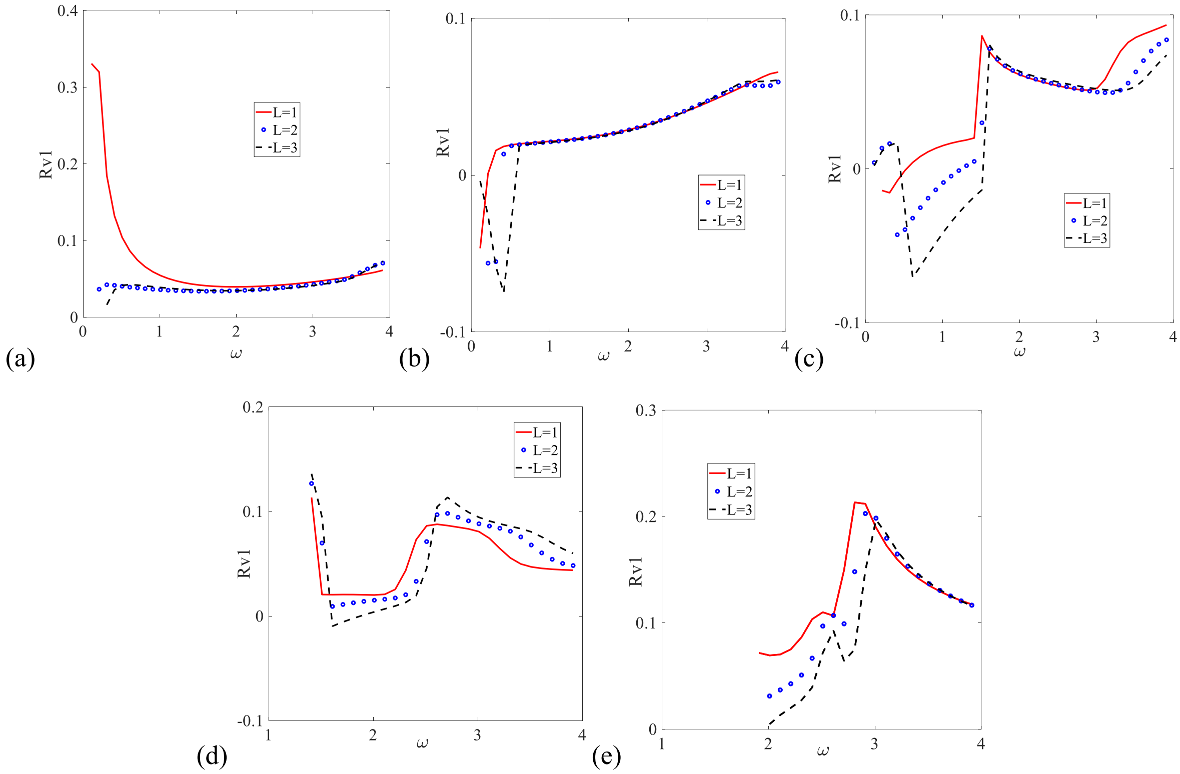

Figure 14. Rv1 of the first five modes with different L, (a)-(e) are the 1st to 5th modes

5.5. Piezoelectric Effect

Fig. 15 shows the piezoelectric effect on the phase velocity and attenuation of the first five flexural waves. The piezoelectric effect increases the phase velocity and attenuation. As mentioned earlier, the nonlocal effect decreases the phase velocity and attenuation. Thus, the nonlocal effect and piezoelectric effect are mutually inhibiting at most frequencies. Meanwhile, the distinguish of the phase velocity and attenuation between the closed and open-circuit conditions mainly occurs at low frequency. For the 4th and 5th modes, the phase velocity and attenuation with open-circuit condition is more significant. Fig.16 displays the intensity of nonlocal effects with different conditions. The intensities of nonlocal effects are influenced by boundary conditions clearly. Without electricity conditions, only a few Rv1 of the 2nd mode are negative. But with electricity conditions, much more Rv1 of the 2nd and 3rd modes are negative. This indicates that the piezoelectric effect exacerbates the strengthening effect at low frequency.

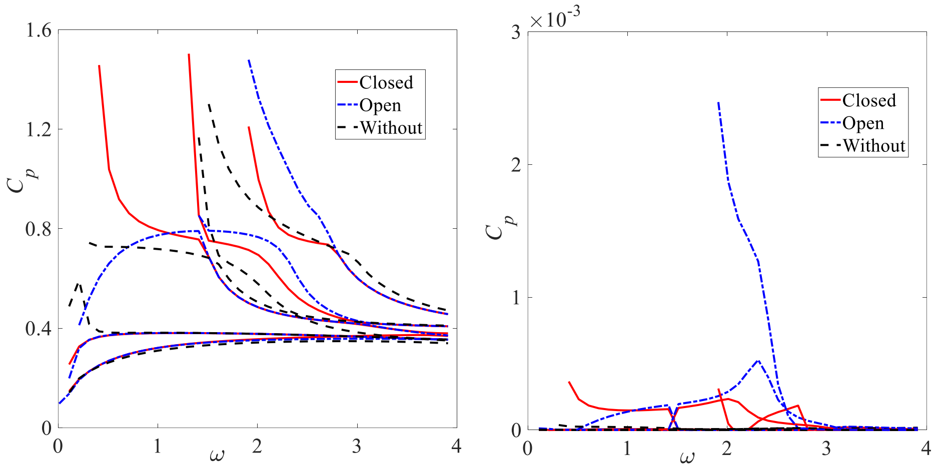

(a) Phase velocity (b) Attenuation

Figure 15. Phase velocity and attenuation of the first five flexural waves with different conditions

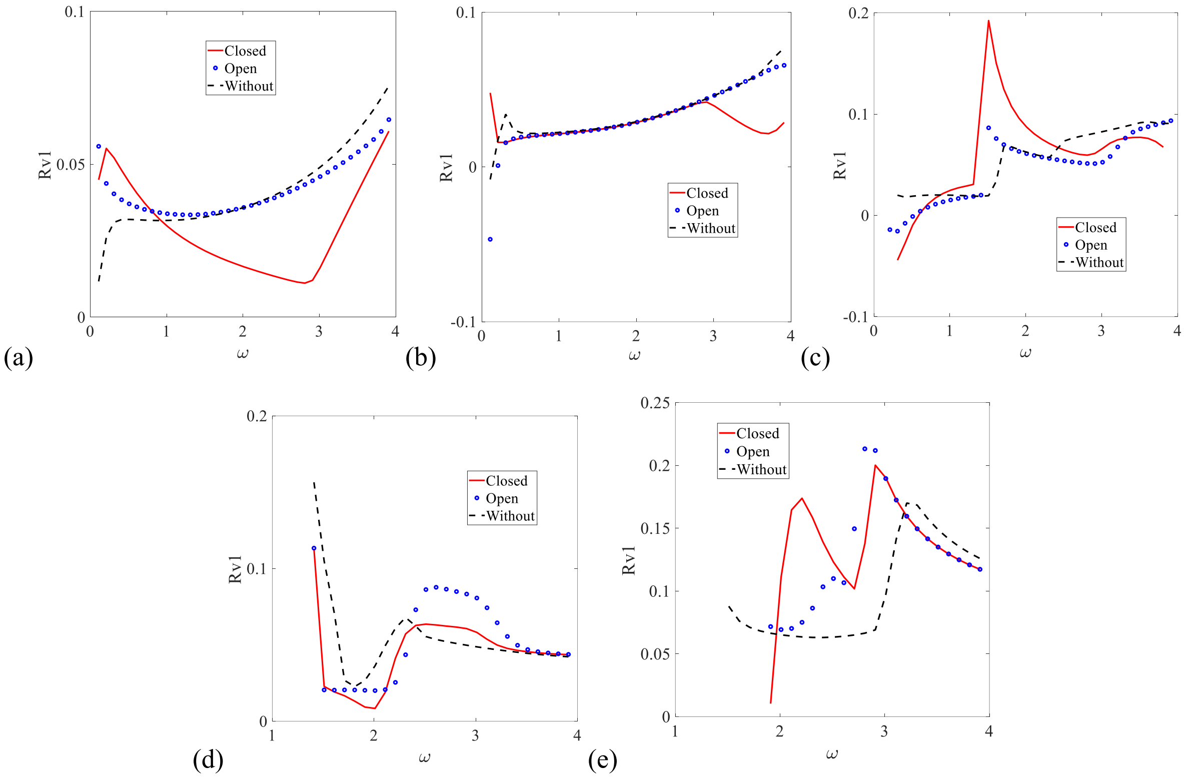

Figure 16. Rv1 of the first five modes with different conditions, (a)-(e) are the 1st to 5th modes

6. Conclusions

In this paper, the thermoelastic wave in FGPM nano hollow cylinders is investigated by using the MNIE. The time-consuming solving process in the integral formulation of MNIE is overcome by the proposed MNIE-LPSA. Reviewing the entire paper, there are the following innovations and findings:

A mathematical model is established for solving the axial thermoelastic wave propagation and attenuation in FGPM nano hollow cylinders by using the MNIE and LPSA.

An efficiently iterative solution method by using the exponential integral function is proposed to solve the difficult to calculate analytically and time-consuming integrals. The computational efficiency can be improved by 99%.

The nonlocal effect increases the attenuation of thermal waves, but decreases the attenuation of the elastic waves. Meanwhile, the nonlocal effect on attenuation is more significant than that on phase velocity.

At low frequencies of the lower-order modes, the nonlocal elasticity displays the strengthening effect. The published results with nonlocal differential elasticity on wave propagation only reflect the softening effect.

For the phase velocity, the nonlocal effect and circumferential order are mutually reinforcing, although the nonlocal effect and piezoelectric effect are mutually inhibiting.

Acknowledgments

This work was supported by the Support by the National Natural Science Foundation of China (No. 12102131), the Key Research Projects in Higher Education Institutions in Henan Province (No. 24A460015), the Innovative research team of Henan Polytechnic University (No. T2022-4), the Henan University Science and Technology Innovation Team Support Plan (No. 23IRTSTHN016).

Conflict of Interest

The authors declare that they have no known competing financial interests or personal relationships that could have appeared to influence the work reported in this paper.

References

[1] Liu Z H, Pan C T, Yen C K, et al. Crystallization and mechanical behavior of the ferroelectric polymer nonwoven fiber fabrics for highly durable wearable sensor applications. Applied Surface Science, 2015, 346: 291-301

[2] Dhua S, Mondal S, Maji A. Surface effects on wave propagation in piezoelectric–piezomagnetic loosely bonded bilayer system using nonlocal theory of elasticity. Thin-Walled Structures, 2024, 197: 111612.

[3] Eringen C A. On differential equations of nonlocal elasticity and solutions of screw dislocation and surface waves. Journal of Applied Physics, 1983, 54(9): 4703-4710.

[4] Wang X H, Ren X Q, Zhou H M, et al.Dynamics of thermoelastic Lamb waves in functionally graded nanoplates based on the modified nonlocal theory. Applied Mathematical Modelling, 2023, 117:142-161.

[5] Lu T Q, Zheng W G, Tang R J, et al. Beam-type acoustic black holes incorporating the microstructure-dependent nonlocal effect. Thin-Walled Structures, 2024, 197: 111662.

[6] Du Y, Zhang J W. Numerical solutions for nonlocal wave equations by perfectly matched layers II: The two-dimensional case. Journal of Computational Physics, 2023, 488: 112209.

[7] Vinh P C, Tuan T T. Harmonic plane waves in isotropic micropolar medium based on two-parameter nonlocal theory. Archive of Applied Mechanics, 2023, 93(9): 3359-3377

[8] Wang S, Wang Y Z. Nonlocal topological states in elastic wave metamaterials with active feedback control. International Journal of Solids and Structures, 2023, 281: 112430.

[9] Wang X H, Chen Y H, Yu J G, et al. Reflection, transmission, and dissipation of plane waves in sandwiched functionally

graded thermo- electro-elastic nanoplates via nonlocal integral elasticity theory. Composite Structures, 2023, 324: 117564.

[10] Romano G, Barretta R, Diaco M. On nonlocal integral models for elastic nano-beams. International Journal of Mechanical Sciences, 2017, 131: 490-499.

[11] Norouzzadeh A , Ansari R , Rouhi H .An analytical study on wave propagation in functionally graded nano-beams/tubes based on the integral formulation of nonlocal elasticity.Waves in Random and Complex Media, 2020, 30(3): 562-580.

[12] Zhang L L, Liu J X, Fang X Q, et al. Effects of surface piezoelectricity and nonlocal scale on wave propagation in piezoelectric nanoplates. European Journal of Mechanics A/solids, 2014, 46(4): 22-29.

[13] Wang X H, Ren X Q, Yu J G, et al. Escape, crossing and cut-off frequencies of SH waves in nonlocal piezoelectric nanoplates.Thin-Walled Structures, 2022, 180: 109982.

[14] Ko J H, Jeong J, Choi J, et al. Quality factor in clamping loss of nanocantilever resonators. Applied Physics Letters, 2011, 98(17): 171909.

[15] Yan D J, Liu R, Zhou J G, et al. Influences of defects on the propagation of transverse waves in periodic piezoelectric laminate structure with nanoscaled layers. Thin-Walled Structures, 2022, 179: 109567.

[16] Li Z N, Liu J, Hu B, et al. Wave propagation analysis of porous functionally graded piezoelectric nanoplates with a visco-Pasternak foundation. Applied Mathematics and Mechanics (English Edition), 2023, 44(1): 35-52.

[17] Li D Z, Li S P, Zhang C L, et al. Propagation characteristics of shear horizontal waves in piezoelectric semiconductor nanoplates incorporating surface effect. International Journal of Mechanical Sciences, 2023, 247: 108201.

[18] Singh B, Sangwan A, Singh J. Reflection and transmission of elastic waves at an interface between two micropolar piezoelectric half-spaces. Journal of Ocean Engineering and Science, 2019, 4(3): 227-237.

[19] Ghayoumizadeh H, Shahabian F, Hosseini S M. Elastic wave propagation in a functionally graded nanocomposite reinforced by carbon nanotubes employing meshless Local Integral Equations (LIEs). Engineering Analysis with Boundary Elements, 2013, 37(11): 1524-1531.

[20] Wang X H, Hou Y Y, Zhang X M, et al.Thermoelastic wave propagation in functionally graded nanohollow cylinders based on nonlocal theory. Journal of the Brazilian Society of Mechanical Sciences and Engineering, 2023, 45: 370.

[21] He D Z, Shi D Y, Wang Q S, et al. Free vibration characteristics and wave propagation analysis in nonlocal functionally graded cylindrical nanoshell using wave-based method. Journal of the Brazilian Society of Mechanical Sciences and Engineering, 2021, 43 (6): 292.

[22] Daneshmand F, Farokhi H, Amabili M. A higher-order mathematical modeling for dynamic behavior of protein microtubule shell structures including shear deformation and small-scale effects. Mathematical Biosciences, 2014, 252: 67-82.

[23] Peng M Q, Li Y, Zhao Y, et al. Transient responses of dielectrics during ultrashort pulsed laser irradiation using a generalized thermoelastic model considering temperature-dependent thermophysical properties. International Journal of Heat and Mass Transfer, 2024, 219: 124884.

[24] Yu J G, Wang X H, Zhang X M, et al. An analytical integration Legendre polynomial series approach for Lamb waves in fractional order thermoelastic multilayered plates. Mathematical Methods in the Applied Sciences. 2022, 45(12): 7631-7651.

[25] Liu Y J, Han Q, Li C L, et al. Guided wave propagation and mode differentiation in the layered magneto-electro-elastic hollow cylinder. Composite Structures, 2015, 132: 558-566.

[26] Zhang X W, Tang Z F, Lu F Z, et al. Excitation of dominant flexural guided waves in elastic hollow cylinders using time delay circular array transducers. Wave Motion, 2016, 62: 41-54

[27] Zhao J G, Liang P H, Yang R J, et al. Thermoelastic wave propagation damping in a hollow FG-GPLRC cylinder with the spinning motion. Thin-Walled Structures, 2022, 177: 109367.

[28] Hosseini S M, Zhang C Z. Coupled thermoelastic analysis of an FG multilayer graphene platelets-reinforced nanocomposite cylinder using meshless GFD method: A modified micromechanical model. Engineering Analysis with Boundary Elements, 2018, 88: 80-92.

[29] Gunawan A, Hirose S. Boundary element analysis of guided waves in a bar with an arbitrary cross-section. Engineering Analysis with Boundary Elements, 2005, 29(10): 913-924.

[30] Sharma J N, Pathania V. Generalized thermoelastic wave propagation in circumferential direction of transversely isotropic cylindrical curved plates. Journal of Sound and Vibration, 2005, 281(3-5): 1117-1131.

[31] Zhang X M, Li Z, Wang X H, et al. The fractional Kelvin-Voigt model for circumferential guided waves in a viscoelastic FGM hollow cylinder. Applied Mathematical Modelling, 2021, 89:299-313.

[32] Wang X H, Li F L, Zhang B, et al. Wave propagation in thermoelastic inhomogeneous hollow cylinders by analytical integration orthogonal polynomial approach. Applied Mathematical Modelling, 2021, 99(7): 57-80.

[33] Lefebvre J E, Zhang V, Gazalet J, et al. Legendre polynomial approach for modeling free-ultrasonic waves in multilayered plates. Journal of Applied Physics, 1999, 85(7): 3419-3427.

[34] Elmaimouni L, Lefebvre J E, Zhang V, et al. Guided waves in radially graded cylinders: a polynomial approach. NDT & E International, 2005, 38(5): 344-353.

[35] Yu J G, Lefebvre J E. Guided waves in multilayered hollow cylinders: the improved Legendre polynomial method. Composite Structures, 2013, 95: 419-429.

[36] Zheng M F, Ma H W, Lyu Y, et al. Derivation of circumferential guided waves equations for a multilayered laminate composite hollow cylinder by state-vector and Legendre polynomial hybrid formalism. Composite Structures, 2020, 255: 112950.

[37] Salehipour H, Shahidi A R, Nahvi H. Modified nonlocal elasticity theory for functionally graded materials[J]. International Journal of Engineering Science, 2015, 90: 44-57.

[38] Sharma J N, Pal M. Propagation of Lamb waves in a transversely isotropic piezothermoelastic plate. Journal of Sound & Vibration, 2004, 270(4-5): 587-610.

[39] Wang Z X, Guo D R. Introduction to special functions. Beijing: Peking University Press, 2014. (in Chinese)

[40] Gradshteyn I S, Ryzhik I M, Jeffrey A. Table of integrals, series, and products. Pittsburgh: Academic Press, 2007.

[41] Arda M. Evaluation of optimum length scale parameters in longitudinal wave propagation on nonlocal strain gradient carbon nanotubes by lattice dynamics. Mechanics Based Design of Structures and Machines, 2022, 50(12): 4363-4386.

[42] Li X Y, Wu J, Ding H J, et al. 3D analytical solution for a functionally graded transversely isotropic piezoelectric circular plate under tension and bending. International Journal of Engineering Science, 2011, 49(7): 664-676.

[43] Guha S, Singh A K. Plane wave reflection/transmission in imperfectly bonded initially stressed rotating piezothermoelastic fiber-reinforced composite half-spaces. European Journal of Mechanics - A/Solids, 2021, 88: 104242.

[44] Rose J L. Ultrasonic Guided Waves in Solid Media. Cambridge: Cambridge University Press, 2014.

Appendix A

All the integrals in the MLPSA are summarized as follows,

$$u_1\left[n,m,j,p,L\right]=\int_a^b\left(\frac{2r-(a+b)}{b-a}\right)^j r^L Q_n(r)\frac{d^p}{dr^p}Q_m(r)dr\,,\quad \text{p=0, 1, 2; L=0, 1, 2;}$$

$$v_1\left[n,m,j,p,L\right]=\int_a^b\left(\frac{2r-(a+b)}{b-a}\right)^j r^L Q_n(r)\frac{d^p}{dr^p}Q_m(r)\frac{\partial H(r)}{\partial r}dr\,,\quad \text{p=0, 1; L=0, 1, 2;}$$

$$u_2[n,m,j,p,q,\gamma,L]=\frac{1}{2\lambda}\int_a^b\left(\frac{2r-(a+b)}{b-a}\right)^j r^L Q_n(r)\frac{d^q}{dr^q}\int_a^b e^{-\frac{|v-r|}{\lambda}}\frac{1}{v^\gamma}\frac{d^p}{dv^p}Q_m(v)dvdr\,,$$

$$v_2[n,m,j,p,q,\gamma,L]=\frac{1}{2\lambda}\int_0^h\left(\frac{2r-(a+b)}{b-a}\right)^j r^L Q_n(r)\frac{\partial H(r)}{\partial r}\frac{d^q}{dr^q}\int_0^h e^{-\frac{|v-r|}{\lambda}}\frac{1}{v^\gamma}\frac{d^p}{dv^p}Q_m(v)dvdr$$

$$u_3[n,m,j,p,q,\gamma,L]=\frac{1}{2\lambda}\int_0^h\left(\frac{2r-(a+b)}{b-a}\right)^j r^L Q_n(r)\frac{d^q}{dr^q}\int_0^h e^{-\frac{|v-r|}{\lambda}}\frac{1}{v^\gamma}\frac{d^p}{dv^p}[(v-a)(v-b)Q_m(v)]dvdr$$

$$v_3[n,m,j,p,q,\gamma,L]=\frac{1}{2\lambda}\int_0^h\left(\frac{2r-(a+b)}{b-a}\right)^j r^L Q_n(r)\frac{\partial H(r)}{\partial r}\frac{d^q}{dr^q}\int_0^h e^{-\frac{|v-r|}{\lambda}}\frac{1}{v^\gamma}\frac{d^p}{dv^p}[(v-a)(v-b)Q_m(v)]dvdr\quad \text{p, q, L, }\gamma = 0,\ 1.$$

$$u_4\left[n,m,j,p,L\right]=\int_a^b\left(\frac{2r-(a+b)}{(b-a)}\right)^j r^L Q_n(r)\frac{d^p}{dr^p}\left[(r-a)(r-b)Q_m(r)\right]dr\,,\quad \text{p=0, 1, 2; L=0, 1, 2;}\quad \text{(A1 a~g)}$$

The detailed expressions of eq.(18a) for coupled waves with electrical open-circuit are given here.

$$\begin{aligned}
A_{11}^{n,m} &= -C_{55}^{(j)}u_2\left[n,m,j,0,0,0,2\right]\\
B_{13}^{n,m} &= iC_{13}^{(j)}u_2\left[n,m,j,0,1,0,2\right]+ijC_{13}^{(j)}u_2\left[n,m,j-1,0,0,0,2\right]+iC_{13}^{(j)}v_2\left[n,m,j,0,0,0,2\right]\\
&\quad +iC_{55}^{(j)}u_2\left[n,m,j,1,0,0,2\right]+i\left(C_{13}^{(j)}-C_{23}^{(j)}\right)u_2\left[n,m,j,0,0,0,1\right]\\
B_{14}^{n,m} &= ie_{31}^{(j)}u_2\left[n,m,j,0,1,0,2\right]+ije_{31}^{(j)}u_2\left[n,m,j-1,0,0,0,2\right]+ie_{31}^{(j)}v_2\left[n,m,j,0,0,0,2\right]\\
&\quad +ie_{15}^{(j)}u_2\left[n,m,j,1,0,0,2\right]+i\left(e_{31}^{(j)}-e_{32}^{(j)}\right)\left[n,m,j,0,0,0,1\right]\\
C_{11}^{n,m} &= C_{11}^{(j)}u_2\left[n,m,j,1,1,0,2\right]+jC_{11}^{(j)}u_2\left[n,m,j-1,1,0,0,2\right]+C_{12}^{(j)}u_2\left[n,m,j,0,1,1,2\right]\\
&\quad +jC_{12}^{(j)}u_2\left[n,m,j-1,0,0,1,2\right]+\left(C_{12}^{(j)}-C_{22}^{(j)}-N^2C_{66}^{(j)}\right)u_2\left[n,m,j,0,0,1,1\right]\\
&\quad +\left(C_{11}^{(j)}-C_{12}^{(j)}\right)u_2\left[n,m,j,1,0,0,1\right]+C_{11}^{(j)}v_2\left[n,m,j,1,0,0,2\right]\\
&\quad +C_{12}^{(j)}v_2\left[n,m,j,0,0,1,2\right]+\omega^2\rho^{(j)}u_1\left[n,m,j,0,2\right]\\
C_{12}^{n,m} &= iN\left(C_{66}^{(j)}u_2\left[n,m,j,1,0,0,1\right]+C_{12}^{(j)}u_2\left[n,m,j,0,1,1,2\right]+jC_{12}^{(j)}u_2\left[n,m,j-1,0,0,1,2\right]\right)\\
&\quad +iNC_{12}^{(j)}v_2\left[n,m,j,0,0,1,2\right]+iN\left(C_{12}^{(j)}-C_{22}^{(j)}-C_{66}^{(j)}\right)u_2\left[n,m,j,0,0,1,1\right]\\
C_{15}^{n,m} &= -\beta_1^{(j)}u_2\left[n,m,j,0,1,0,2\right]-j\beta_1^{(j)}u_2\left[n,m,j-1,0,0,0,2\right]-\beta_1^{(j)}v_2\left[n,m,j,0,0,0,2\right]\\
&\quad -\left(\beta_2^{(j)}-\beta_1^{(j)}\right)u_2\left[n,m,j,0,0,0,1\right]
\end{aligned}$$

$$A_{22}^{n,m} = -k^2 C_{44}^{(j)} u_2\left(n,m,j,0,0,0,2\right)$$
$$B_{23}^{n,m} = -NC_{23}^{(j)} u_2\left(n,m,j,0,0,0,1\right) - NC_{44}^{(j)} u_2\left(n,m,j,0,0,1,2\right)$$
$$B_{24}^{n,m} = -Ne_{32}^{(j)} u_2\left(n,m,j,0,0,0,1\right) - Ne_{24}^{(j)} u_2\left(n,m,j,0,0,1,2\right)$$

$$\begin{aligned}C_{21}^{n,m} = {}& iNC_{66}^{(j)} u_2\left(n,m,j,0,1,1,2\right) + ijNC_{66}^{(j)} u_2\left(n,m,j-1,0,0,1,2\right) + iNC_{66}^{(j)} v_2\left(n,m,j,0,0,1,2\right) \\ & + iNC_{12}^{(j)} u_2\left(n,m,j,1,0,0,1\right) + iNC_{22}^{(j)} u_2\left(n,m,j,0,0,1,1\right) + 2iNC_{22}^{(j)} u_2\left(n,m,j,0,0,1,1\right)\end{aligned}$$

$$\begin{aligned}C_{22}^{n,m} = {}& C_{66}^{(j)} u_2\left(n,m,j,1,1,0,2\right) - C_{66}^{(j)} u_2\left(n,m,j,0,1,1,2\right) + C_{66}^{(j)} v_2\left(n,m,j,1,0,0,2\right) \\ & + jC_{66}^{(j)} u_2\left(n,m,j-1,1,0,0,2\right) - jC_{66}^{(j)} u_2\left(n,m,j-1,0,0,1,2\right) - C_{66}^{(j)} v_2\left(n,m,j,0,0,1,2\right) \\ & - N^2 C_{22}^{(j)} u_2\left(n,m,j,0,0,1,1\right) + 2C_{66}^{(j)} u_2\left(n,m,j,1,0,0,1\right) \\ & - 2C_{66}^{(j)} u_2\left(n,m,j,0,0,1,1\right) + \omega^2 \rho^{(j)} u_1\left(n,m,j,0,2\right)\end{aligned}$$

$$C_{25}^{n,m} = -iN\beta_2^{(j)} u_2\left(n,m,j,0,0,0,1\right)$$

$$A_{33}^{n,m} = -C_{33}^{(j)} u_2\left(n,m,j,0,0,0,2\right)$$
$$A_{34}^{n,m} = -e_{33}^{(j)} u_2\left(n,m,j,0,0,0,2\right)$$
$$\begin{aligned}B_{31}^{n,m} = {}& iC_{55}^{(j)} u_2\left(n,m,j,0,1,0,2\right) + ijC_{55}^{(j)} u_2\left(n,m,j-1,0,0,0,2\right) + iC_{55}^{(j)} v_2\left(n,m,j,0,0,0,2\right) \\ & + iC_{13}^{(j)} u_2\left(n,m,j,1,0,0,2\right) + iC_{23}^{(j)} u_2\left(n,m,j,0,0,1,2\right) + iC_{55}^{(j)} u_2\left(n,m,j,0,0,0,1\right)\end{aligned}$$
$$B_{32}^{n,m} = -NC_{44}^{(j)} u_2\left(n,m,j,0,0,0,1\right) - NC_{23}^{(j)} u_2\left(n,m,j,0,0,1,2\right)$$
$$B_{35}^{n,m} = -i\beta_3^{(j)} u_2\left(n,m,j,0,0,0,2\right)$$
$$\begin{aligned}C_{33}^{n,m} = {}& C_{55}^{(j)} u_2\left(n,m,j,1,1,0,2\right) + jC_{55}^{(j)} u_2\left(n,m,j-1,0,1,0,2\right) + C_{55}^{(j)} v_2\left(n,m,j,1,0,0,2\right) \\ & - N^2 C_{44}^{(j)} u_2\left(n,m,j,0,0,1,1\right) + C_{55}^{(j)} u_2\left(n,m,j,1,0,0,1\right) + \omega^2 \rho^{(j)} u_2\left(n,m,j,0,2\right)\end{aligned}$$
$$\begin{aligned}C_{34}^{n,m} = {}& e_{15}^{(j)} u_2\left(n,m,j,1,1,0,2\right) + je_{15}^{(j)} u_2\left(n,m,j-1,0,1,0,2\right) + e_{15}^{(j)} v_2\left(n,m,j,1,0,0,2\right) \\ & - N^2 e_{24}^{(j)} u_2\left(n,m,j,0,0,1,1\right) + e_{15}^{(j)} u_2\left(n,m,j,1,0,0,1\right)\end{aligned}$$

$$A_{43}^{n,m} = -e_{33}^{(j)} u_2\left(n,m,j,0,0,0,2\right)$$
$$A_{44}^{n,m} = \in_{33}^{(j)} u_2\left(n,m,j,0,0,0,2\right)$$
$$\begin{aligned}B_{41}^{n,m} = {}& ie_{15}^{(j)} u_2\left(n,m,j,0,1,0,2\right) + ije_{15}^{(j)} u_2\left(n,m,j-1,0,0,0,2\right) + ie_{15}^{(j)} v_2\left(n,m,j,0,0,0,2\right) \\ & + ie_{31}^{(j)} u_2\left(n,m,j,1,0,0,2\right) + ie_{32}^{(j)} u_2\left(n,m,j,0,0,1,2\right) + ie_{15}^{(j)} u_2\left(n,m,j,0,0,0,1\right)\end{aligned}$$
$$B_{42}^{n,m} = -Ne_{32}^{(j)} u_2\left(n,m,j,0,0,1,2\right) - Ne_{24}^{(j)} u_2\left(n,m,j,0,0,0,1\right)$$
$$\begin{aligned}C_{43}^{n,m} = {}& e_{15}^{(j)} u_2\left(n,m,j,1,1,0,2\right) + je_{15}^{(j)} u_2\left(n,m,j-1,1,0,0,2\right) + e_{15}^{(j)} v_2\left(n,m,j,1,0,0,2\right) \\ & + e_{15}^{(j)} u_2\left(n,m,j,1,0,0,1\right) - N^2 e_{24}^{(j)} u_2\left(n,m,j,0,0,1,1\right)\end{aligned}$$
$$\begin{aligned}C_{44}^{n,m} = {}& -\in_{11}^{(j)} u_2\left(n,m,j,1,1,0,2\right) - j\in_{11}^{(j)} u_2\left(n,m,j-1,1,0,0,2\right) - \in_{11}^{(j)} v_2\left(n,m,j,1,0,0,2\right) \\ & - \in_{11}^{(j)} u_2\left(n,m,j,1,0,0,1\right) + N^2 \in_{22}^{(j)} u_2\left(n,m,j,0,0,1,1\right)\end{aligned}$$
$$\begin{aligned}C_{45}^{n,m} = {}& P_3^{(j)} u_2\left(n,m,j,0,1,0,2\right) + jP_3^{(j)} u_2\left(n,m,j-1,0,0,0,2\right) \\ & + P_3^{(j)} v_2\left(n,m,j,0,0,0,2\right) + P_3^{(j)} u_2\left(n,m,j,0,0,0,1\right)\end{aligned}$$

$$A_{55}^{n,m} = -K_3^{(j)} u_3\left(n,m,j,0,0,0,2\right)$$
$$B_{53}^{n,m} = -\omega\eta\beta_3^{(j)}\left(1-i\omega\right)u_2\left(n,m,j,0,0,0,2\right)$$
$$B_{54}^{n,m} = \omega\eta P_3^{(j)}\left(1-i\omega\right)u_2\left(n,m,j,0,0,0,2\right)$$
$$C_{51}^{n,m} = i\omega\eta\beta_1^{(j)}\left(1-i\omega\right)u_2\left(n,m,j,1,0,0,2\right) + i\omega\eta\beta_2^{(j)}\left(1-i\omega\right)u_2\left(n,m,j,0,0,1,2\right)$$
$$C_{52}^{n,m} = -N\omega\eta\beta_2^{(j)}\left(1-i\omega\right)u_2\left(n,m,j,0,0,1,2\right)$$
$$\begin{aligned} C_{55}^{n,m} &= K_1^{(j)} u_2\left(n,m,j,0,2,0,2\right) - N^2 K_2^{(j)} u_2\left(n,m,j,0,0,0,0\right) + K_2^{(j)} u_2\left(n,m,j,0,1,0,1\right) \\ &\quad + i\omega\rho^{(j)} C_e^{(s)}\left(1-i\omega\right)u_2\left(n,m,j+s,0,2\right) \end{aligned}$$

The addition operation is performed when j or s appears more than once.

The distinctive expressions of coupled waves with electrical closed-circuit are shown as follows.

$$\begin{aligned} B_{14}^{n,m} &= ie_{31}^{(j)} u_3\left[n,m,j,0,1,0,2\right] + ije_{31}^{(j)} u_3\left[n,m,j-1,0,0,0,2\right] + ie_{31}^{(j)} v_3\left[n,m,j,0,0,0,2\right] \\ &\quad + ie_{15}^{(j)} u_3\left[n,m,j,1,0,0,2\right] + i\left(e_{31}^{(j)} - e_{32}^{(j)}\right) u_3\left[n,m,j,0,0,0,1\right] \end{aligned}$$

$$B_{24}^{n,m} = -Ne_{32}^{(j)} u_3\left(n,m,j,0,0,0,1\right) - Ne_{24}^{(j)} u_3\left(n,m,j,0,0,1,2\right)$$

$$A_{34}^{n,m} = -e_{33}^{(j)} u_3\left(n,m,j,0,0,0,2\right)$$

$$A_{44}^{n,m} = \in_{33}^{(j)} u_3\left(n,m,j,0,0,0,2\right)$$
$$\begin{aligned} B_{41}^{n,m} &= ie_{15}^{(j)} u_2\left(n,m,j,0,1,0,2\right) + ije_{15}^{(j)} u_2\left(n,m,j-1,0,0,0,2\right) \\ &\quad + ie_{31}^{(j)} u_2\left(n,m,j,1,0,0,2\right) + ie_{32}^{(j)} u_2\left(n,m,j,0,0,1,2\right) + ie_{15}^{(j)} u_2\left(n,m,j,0,0,0,1\right) \end{aligned}$$
$$\begin{aligned} C_{43}^{n,m} &= e_{15}^{(j)} u_2\left(n,m,j,1,1,0,2\right) + je_{15}^{(j)} u_2\left(n,m,j-1,1,0,0,2\right) \\ &\quad + e_{15}^{(j)} u_2\left(n,m,j,1,0,0,1\right) - N^2 e_{24}^{(j)} u_2\left(n,m,j,0,0,1,1\right) \end{aligned}$$
$$\begin{aligned} C_{44}^{n,m} &= -\in_{11}^{(j)} u_3\left(n,m,j,1,1,0,2\right) - j\in_{11}^{(j)} u_3\left(n,m,j-1,1,0,0,2\right) \\ &\quad - \in_{11}^{(j)} u_3\left(n,m,j,1,0,0,1\right) + N^2 \in_{22}^{(j)} u_3\left(n,m,j,0,0,1,1\right) \end{aligned}$$
$$C_{45}^{n,m} = P_3^{(j)} u_2\left(n,m,j,0,1,0,2\right) + jP_3^{(j)} u_2\left(n,m,j-1,0,0,0,2\right) + P_3^{(j)} u_2\left(n,m,j,0,0,0,1\right)$$

$$B_{54}^{n,m} = \omega\eta P_3^{(j)}\left(1-i\omega\right)u_3\left(n,m,j,0,0,0,2\right)$$